European Journal of Medicinal Chemistry 265 (2024) 116125

Contents lists available at ScienceDirect

European Journal of Medicinal Chemistry

journal homepage: www.elsevier.com/locate/ejmech

Research paper

Benzopyran hydrazones with dual PPARα/γ or PPARα/δ agonism and an anti-inflammatory effect on human THP-1 macrophages

Ainhoa García [a,b], Laura Vila [b], Isabelle Duplan [c], María Ayelén Schiel [d], Ricardo D. Enriz [d], Nathalie Hennuyer [c,**], Bart Staels [c], Nuria Cabedo [a,b,*], Diego Cortes [a]

[a] Department of Pharmacology, University of Valencia, 46100, Burjassot, Valencia, Spain
[b] Institute of Health Research-INCLIVA, University Clinic Hospital of Valencia, 46010, Valencia, Spain
[c] Univ. Lille, Inserm, CHU Lille, Institut Pasteur de Lille, U-1011-EGID, F-59000, Lille, France
[d] Faculty of Chemistry, Biochemistry and Pharmacy, National University of San Luis-IMIBIO-SL-CONICET, Chacabuco, 917-5700, San Luis, Argentina

ARTICLE INFO

Keywords:
Benzopyran hydrazones
Synthesis
Molecular modelling
PPAR agonists
Anti-inflammatory activity
Cytotoxicity

ABSTRACT

Peroxisome proliferator-activated receptors (PPARs) play a major role in regulating inflammatory processes, and dual or pan-PPAR agonists with PPARγ partial activation have been recognised to be useful to manage both metabolic syndrome and metabolic dysfunction-associated fatty liver disease (MAFLD). Previous works have demonstrated the capacity of 2-prenylated benzopyrans as PPAR ligands. Herein, we have replaced the isoprenoid bond by hydrazone, a highly attractive functional group in medicinal chemistry. In an attempt to discover novel and safety PPAR activators, we efficiently prepared benzopyran hydrazone/hydrazine derivatives containing benzothiazole *(series 1)* or 5-chloro-3-(trifluoromethyl)-2-pyridine moiety (*series 2*) with a 3- or 7-carbon side chain at the 2-position of the benzopyran nucleus. Benzopyran hydrazones **4** and **5** showed dual hPPARα/γ agonism, while hydrazone **14** exerted dual hPPARα/δ agonism. These three hydrazones greatly attenuated inflammatory markers such as IL-6 and MCP-1 on the THP-1 macrophages *via* NF-κB activation. Therefore, we have discovered novel hits (**4**, **5** and **14**), containing a hydrazone framework with dual PPARα/γ or PPARα/δ partial agonism, depending on the length of the side chain. Benzopyran hydrazones emerge as potential lead compounds which could be useful for treating metabolic diseases.

1. Introduction

Peroxisome proliferator-activated receptors (PPARs) are members of the nuclear receptor superfamily of transcription factors, comprising three isotypes [PPARα (NR1C1), PPARβ/δ (NR1C2) and PPARγ (NR1C3)] which have different tissue distribution, ligand specificities, and metabolic regulatory activities [1,2]. In structural terms, PPARs contain a DNA-binding domain (DBD) in the N-terminus and a ligand-binding domain (LBD) in the C-terminus. The DBD sets the binding with PPAR response elements (PPREs) in specific regions of the target genes and the LBD forms the pocket for direct interaction with specific ligands. After the interaction with ligands, PPARs are translocated to the nucleus and heterodimerise with the retinoid X receptor (RXR) to form the PPAR-RXR complex. PPAR-RXR binding by agonists induces the recruitment of coactivators (e.g., CBP or p300) and the release of corepressors (e.g., NCoR or SMRT) by stimulating the gene transcription of the target genes [3–5]. The three PPAR isoforms are involved in fatty acid oxidation, glucose metabolism, and lipid metabolism. PPARα is expressed mainly in the tissues involved in increased fatty acid oxidation, such as liver, skeletal muscle and heart, and controls lipid metabolism. PPARα activation decreases triglyceride levels in plasma and increases HDL-c to play a significant role in the treatment of dyslipidaemia [6]. PPARα is also implicated in glucose homeostasis and insulin resistance [7,8]. PPARβ/δ is ubiquitous, but is highly expressed in those tissues involved in fatty acid metabolism, such as skeletal and cardiac muscle, hepatocytes and adipocytes. Its activation improves insulin sensitivity and the plasma lipid profile, which may manage both dyslipidaemia and type 2 diabetes, although no PPARβ/δ agonist has yet been approved for clinical use [9]. PPARγ is widely expressed in adipose tissue and its activation is related to adipogenesis, lipid storage, insulin sensitivity and glucose homeostasis. Its agonists have been widely used for treating type 2 diabetes. However, much evidence indicates that

* Corresponding author. Department of Pharmacology, University of Valencia, 46100, Burjassot, Valencia, Spain.
** Corresponding author.
E-mail addresses: nathalie.hennuyer@pasteur-lille.fr (N. Hennuyer), ncabedo@uv.es (N. Cabedo), dcortes@uv.es (D. Cortes).

https://doi.org/10.1016/j.ejmech.2024.116125
Received 13 July 2023; Received in revised form 2 January 2024; Accepted 3 January 2024
Available online 4 January 2024

potent and full PPARγ activators are related with serious adverse effects, and a partial agonism would lead to safer drugs [2]. The endogenous ligands for PPARs are fatty acids, cyclooxygenase-derived eicosanoids and prostaglandins, as well as their metabolites. The most known synthetic ligands are fibrates and WY-14,643, GW501516 or rosiglitazone (thiazolidinedione) (Fig. 1), which act as strong agonists for PPARα, PPARβ/δ or PPARγ, respectively [10]. In addition, the three isoforms (α, β/δ, γ) play a major role in regulating inflammatory processes, and have been recognised as the target for the management of metabolic syndrome, obesity, dyslipidaemia, type 2 diabetes, atherosclerosis [2,4], and metabolic dysfunction-associated fatty liver disease (MAFLD). They are all accompanying with a persistent chronic, low-grade inflammation state in several tissues, including adipose tissue, pancreatic islets and liver [11]. Macrophages are phagocytic innate immune cells involved in immunity, tissue remodelling and lipid homeostasis. These immune cells are present in all tissues and play a crucial role during the development of metabolic disorders [11–13] and associated inflammation. The three PPAR isoforms are highly expressed in human macrophages [13], whose function can be regulated by PPAR agonists to prevent metabolic diseases. Infiltrate macrophages in tissues also release pro-inflammatory cytokines and chemokines, which contribute to an inflammation state. Of them, monocyte chemoattractant protein-1 (MCP-1/CCL2) is an important chemokine that is implicated in both the recruitment and activation of monocytes [14], and its down-regulation has been found to occur with improvement of metabolic disorders [15,16]. Interleukin 6 (IL-6) is an inflammatory cytokine IL-6 whose overproduction is directly related to obesity, diabetes and progression to metabolic and cardiovascular disorders [17]. PPAR agonists have been reported to suppress the immunoreactive state of macrophages by the suppression of immune reactive cytokine and chemokines markers, including MCP-1 and IL-6 [2,18].

In 1995, our research group isolated polycerasoidol from the stem bark *of Polyalthia cerasoides* (Annonaceae) [19] (Fig. 1). This 2-prenylated benzopyran contains the chroman-6-ol nucleus like the PPARγ agonist troglitazone (Fig. 1), two isoprenoid units and a terminal carboxylic group on the side chain at 2-position. Polycerasoidol displayed potent dual PPARα/γ agonism and anti-inflammatory effects by inhibiting mononuclear cell-endothelium interactions in a dysfunctional endothelium [20]. Polycerasoidol became the first-in-class with potential to manage several of the risk factors involved in the development of

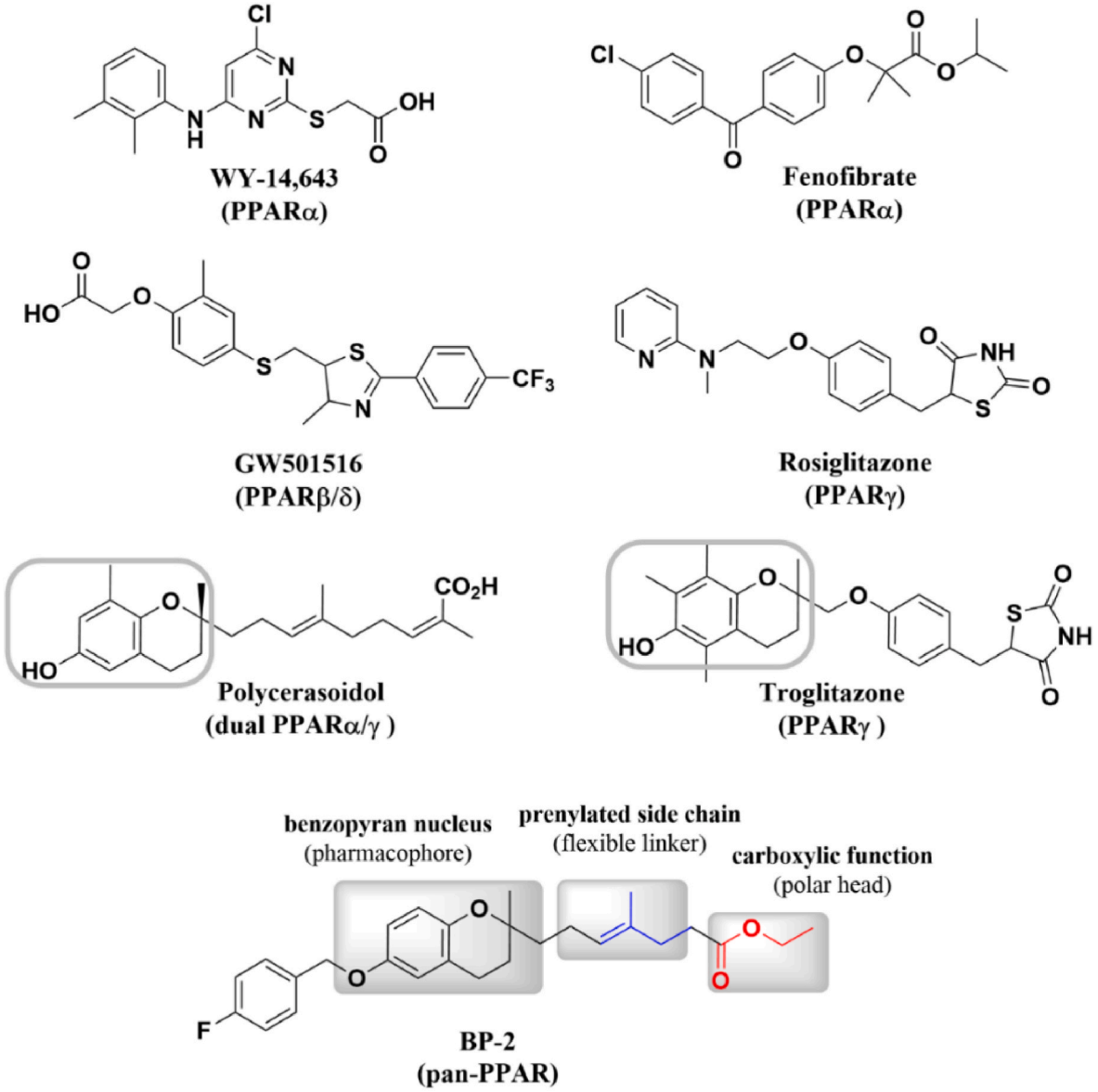

Fig. 1. Synthetic ligands, and natural or synthetic benzopyrans as PPAR agonists.

metabolic syndrome. Next, we carried out structure-activity relationship (SAR) studies of synthetic polycerasoidol analogues and molecular modelling study analyses to explore those key structural features implicated in the modulation of PPARs [21–23]. These studies have indicated that: i) the oxygen atom at 6-position in the benzopyran nucleus (pharmacophore); ii) the length of the prenylated side chain (flexible linker) from 5- to 11-carbons; iii) ester, amide and *O*-alkoxylated bioisosters in the carboxylic function (polar head) can improve hPPARα and hPPARγ interactions. A recent hit-to-lead strategy identified 2-(ethyl-4-′-methylhept-4′-enoate)-6-(*p*-fluorobenzyloxy)-2-(methyl)-benzodihydropyran (BP-2) (Fig. 1) as a pan-PPAR with PPARγ partial activation, and capable of ameliorating metabolic alterations in an obese and diabetic mouse model (*ob/ob* mice) [24].

On the other hand, hydrazone (-CH═N–NH-) and hydrazine (–CH–N–NH–) functions are present in many bioactive natural and synthetic compounds [25–29], attracting the interest as privilege moieties in medicinal chemistry. Among them, the antibiotic rifampicin and the antiparasitic nifurtimox (anti-parasitic drug for Chagas disease) contain the hydrazone moiety, while the hydrazine group is found in the antihypertensive hydralazine (vasodilator), the antidepressant phenelzine (monoamine oxidase inhibitor) and the anticancer procarbazine, all of which are clinically used drugs (Fig. 2). Synthesised hydrazones were also reported to display antidyslipidaemic and antidiabetic activities by different mechanisms [30,31]. In addition, heterocyclic systems are valuable scaffolds to design new therapeutic derivatives. Benzo[*d*]thiazole moiety is found in lanifibranor (Fig. 3), a pan-PPAR agonist and the first drug clinically approved for MAFLD, whereas pyridyl fragment is present in rosiglitazone (Fig. 1) and pioglitazone (Fig. 3), two thiazolidinediones with full PPARγ agonism and used as anti-diabetic agents.

Based on our previous works on 2-prenylated benzopyrans, and in a view of discovering novel chemical entities with dual- or pan-PPAR agonism, but with PPARγ partial agonism to avoid adverse effects associated to a full and selective PPARγ activation, we have explored the possibility to replace both the isoprenyl (flexible linker) and the ethyl carboxylate (polar head) moieties by potential bioisosters. Herein, we have synthesised and evaluated the PPAR activity of novel benzopyrans (pharmacophore) containing in the hydrocarbon side chain at 2-position a hydrazone or hydrazine (its reduced form) function linked to a heterocyclic system such as benzothiazole or 5-chloro-3-(trifluoromethyl)-2-pyridine, two attractive templates for PPAR target (Fig. 3). The anti-inflammatory potential of synthesised compounds was also evaluated *in vitro* in terms of modulating the expression of MCP-1 and IL-6 in human THP-1 macrophages under inflammatory conditions. Accordingly, we have identified novel hits as potential drugs to develop lead candidates which could be useful for metabolic syndrome, type 2 diabetes, dyslipidaemia, MAFLD or inflammation, which can further progress to microvascular problems and cardiovascular events, primary causes of morbidity and death worldwide [32].

2. Results and discussion

2.1. Synthesis of benzopyran hydrazones

We prepared two series of benzopyran hydrazones/hydrazines containing benzothiazole moiety (*series 1*) or 1-[5-chloro-3-(trifluoromethyl)-2-pyridyl] (*series 2*). The benzopyran nucleus was synthesised *via* a chroman-4-one scaffold, which was obtained by the aldol condensation between an *ortho*-hydroxyacetophenone and a ketone in the presence of a secondary amine by Michael addition as previously reported [21–23]. The reaction started with the condensation between 2,5-dihydroxyacetophenone and ethyl levulinate as the proper ketone in the presence of pyrrolidine (Scheme 1). Then, the γ-benzopyrone was reduced under Clemmensen conditions using dust zinc in acid medium to afford the benzodihydropyran **1**, and its phenolic group was protected utilising *p*-fluorobenzyl chloride in the presence of potassium carbonate to give the *p*-fluorobenzyloxy benzodihydropyran **2**. The controlled reduction of the ester function of benzopyran **2** using DIBAL-H reagent allowed us to obtain the aldehyde intermediate **3**.

In a first approach, we prepared benzopyran hydrazones with a 3-carbon side chain. For this purpose, aldehyde intermediate **3** condensed with the available hydrazines such as 2-hydrazinobenzothiazole and 1-[5-chloro-3-(trifluoromethyl)-2-pyridyl]hydrazine in anhydrous dichloroethane gave imines (Schiff bases) with hydrazone moieties **4** (*series 1*) and **5** (*series 2*), respectively [33]. Deprotection of compounds **4** and **5** with

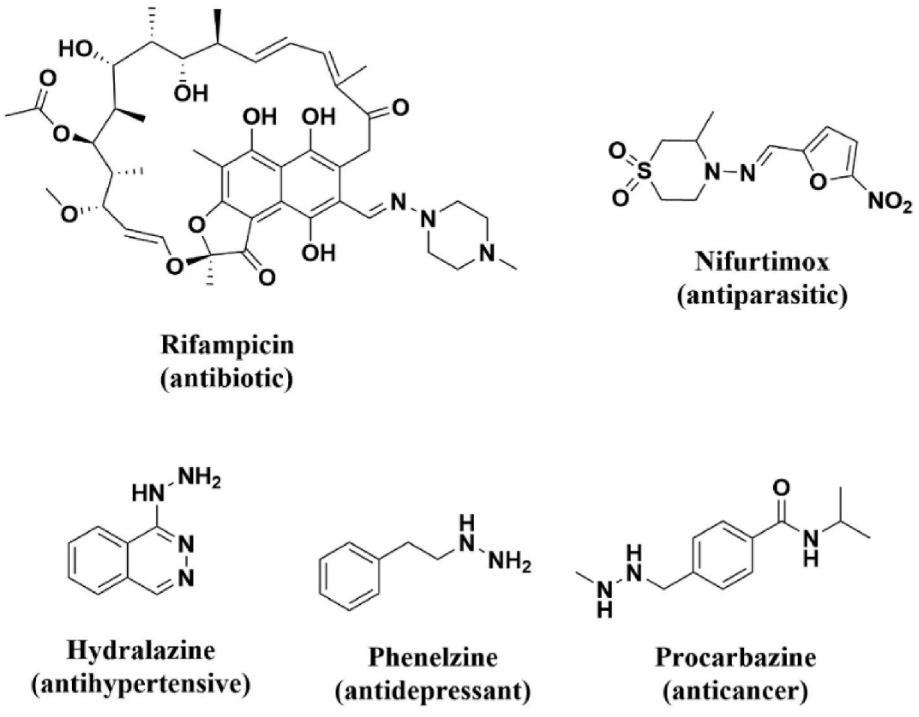

Fig. 2. Clinical drugs containing hydrazone (C═N–NH) or hydrazine (NH–NH) moiety.

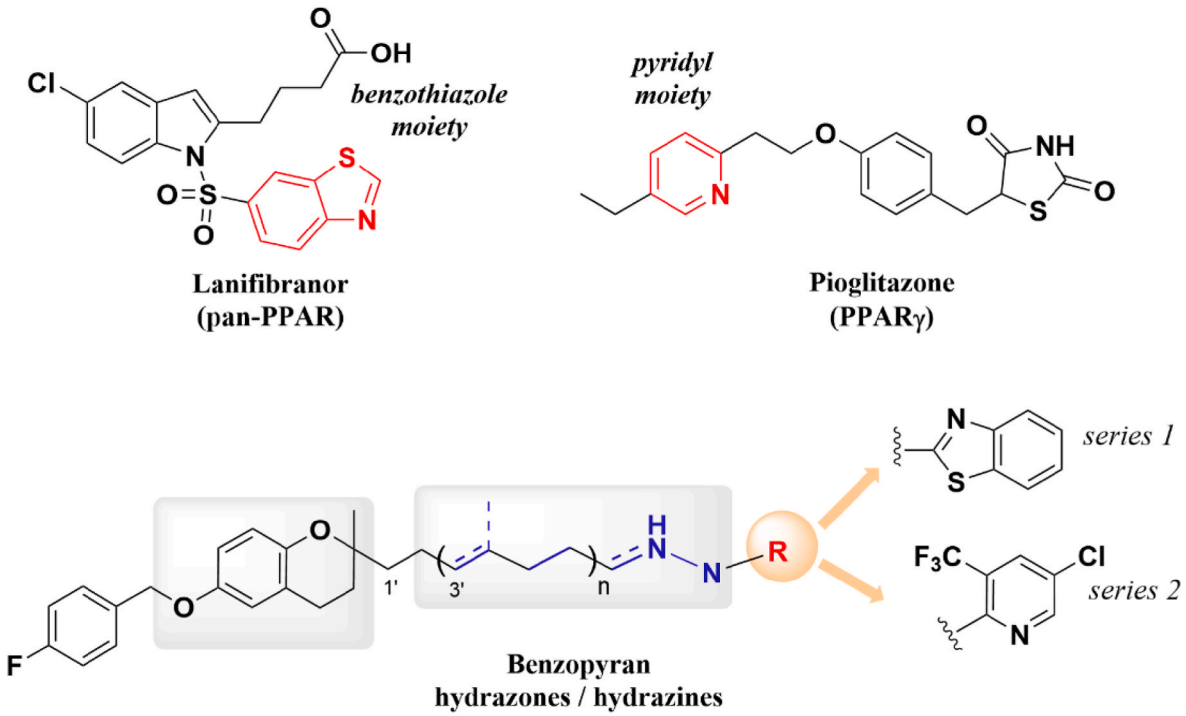

Fig. 3. Clinical drugs and designed benzopyran hydrazones/hydrazines containing benzothiazole or pyridinyl moiety.

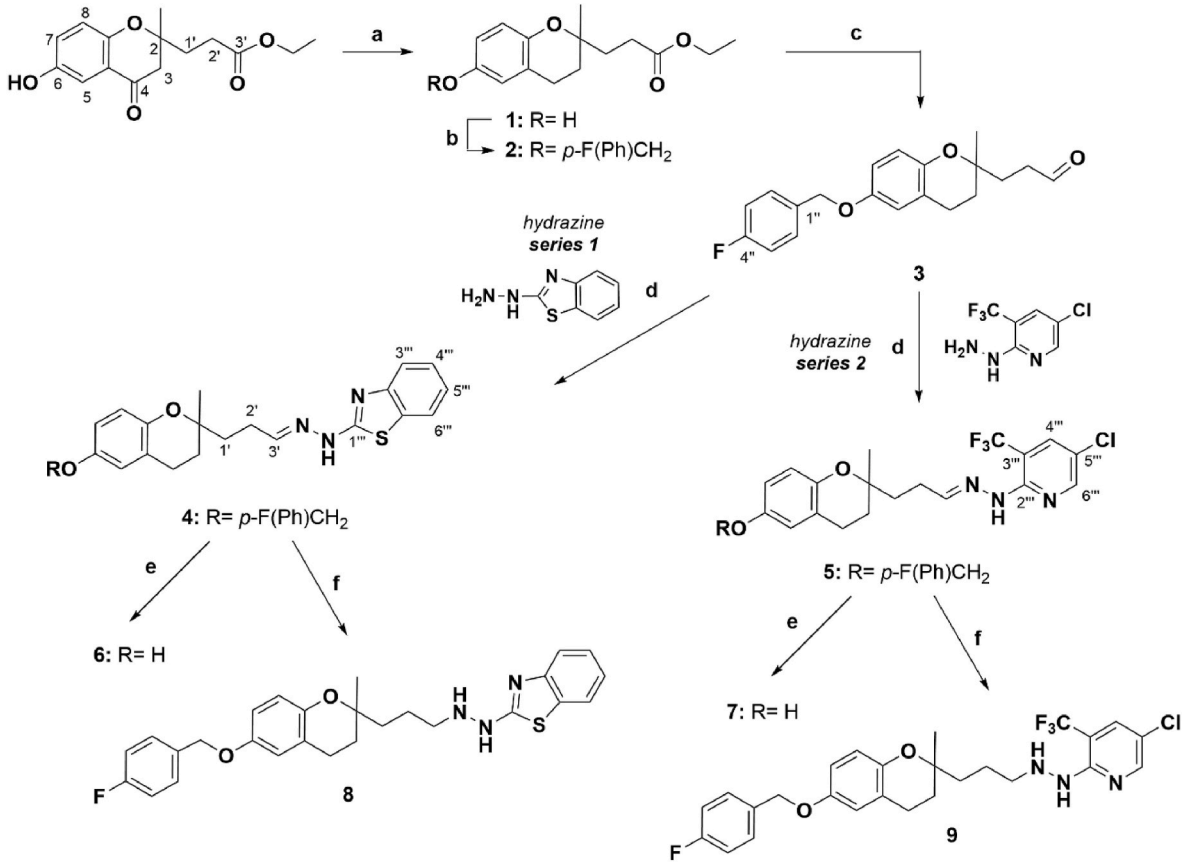

Scheme 1. Synthesis of 2-substituted benzopyrans containing hydrazone/hydrazine moiety. *Reagents and conditions*: (a) Zn dust/conc HCl, AcOH-H_2O (2:1, v/v), r.t, 1 h 30 min (58%); (b) *p*-fluorobenzyl chloride, K_2CO_3, EtOH, reflux, 4 h (79%); (c) 1 M DIBAL-H in THF, CH_2Cl_2, -78 °C, N_2, 15 min (92%); (d) hydrazines: 2-hydrazinobenzothiazole or 1-[5-Cl-3-(CF_3-2-pyridyl]$NHNH_2$), $(CH_2)_2Cl_2$, r.t, N_2, 1 h (80% for **4**; 89% for **5**); (e) BBr_3, CH_2Cl_2, r.t, N_2, 1 h (91% for **6**; 92% for **7**); (f) $NaBH_4CN$, BF_3OEt, MeOH, N_2, reflux, 1 h (96% for **8**; 75% for **9**).

boron tribromide afforded compounds **6** (*series 1*) and **7** (*series 2*), respectively, bearing both a hydrazone moiety and a free phenolic group (Scheme 1) [34]. The reduction of the imine double bond in hydrazones (-C═NH–NH-) to attain hydrazines (–CH_2–NH–NH–) has been reported by catalytic hydrogenation under high pressure or hydride reductions, including lithium aluminium hydride [35], sodium borohydride in Raney nickel [36], sodium cyanoborohydride [37], the borane trimethylamine complex in hydrochloric acid [38] and magnesium in methanol [39], which are usually tedious or inefficient procedures. In our approach, hydrazones were reduced using a methodology previously reported to reduce quinolines to tetrahydroquinolines [40]. Thus, benzopyran hydrazines **8** (*series 1*) and **9** (*series 2*) were easily and efficiently prepared from their hydrazones **4** and **5**, respectively, by sodium cyanoborohydride and boron trifluoride etherate as catalyst to generate diborane *in situ* (Scheme 1).

In a second approach, we synthesised two series of benzopyran hydrazones with a 7-carbon side chain (C-1′ to C-7′) instead of 3-carbons (C-1′ to C-3′). The elongation of the hydrocarbon side chain from aldehyde **3** was performed by an efficient Grignard reaction, followed by Johnson-Claisen rearrangement to obtain benzopyran ester **11** [21,22,24]. The Grignard reaction consisted in the nucleophilic attack of propenyl magnesium bromide to the electrophilic carbon of aldehyde **3** to form a carbon-carbon bond. The Johnson-Claisen rearrangement of allylic alcohol intermediate **10** was carried out using 1,1,1-triethoxyethane and catalytic amounts of isobutyric acid. Then benzopyran ester **11** was subjected to controlled reduction with DIBAL-H reagent to give aldehyde **12**. The condensation of aldehyde **12** with the corresponding hydrazines, such as 2-hydrazinobenzothiazole and 1-[5-chloro-3-(trifluoromethyl)-2-pyridyl]hydrazine in anhydrous dichloroethane gave benzopyran hydrazones **13** (*series 1*) and **14** (*series 2*), respectively (Scheme 2).

2.2. PPARα, PPARβ/δ and PPARγ agonist activity

All the synthetized compounds were assayed *in vitro* for hPPARα, hPPARβ/δ or hPPARγ transcriptional activity by a cell-based transactivation assay in Cos-7 cells properly transfected with a luciferase-reported plasmid in the presence of expression vectors pGAL4hPPARα, pGAL4hPPARβ/δ and pGAL4hPPARγ [24]. The activity of each compound was expressed as each compound' percentage of efficacy at 10 μM by comparing to the maximal efficacy of the reference compounds: WY-14,643 (at 10 μM), rosiglitazone (at 1 μM) or GW501516 (at 1 μM) as hPPARα, hPPARγ or hPPARβ/δ respectively. Half maximal effective concentration EC_{50} was calculated by using the Prism software (Table 1). The results showed that benzopyran hydrazones **4** (*series 1*) and **5** (*series 2*) at 10 μM displayed dual hPPARα/γ partial activation. It was noteworthy that hydrazone framework, instead of the isoprenyl, also exerts a PPAR activity providing a new class of benzopyran agonists. Benzopyran hydrazone **14** (*series 2*), bearing an elongated 7-carbon side chain with an isoprenoid unit and

Table 1
Evaluation of agonist activity in a cell-based transactivation assays for human PPAR/Gal_4 receptors. EC_{50} values against human PPARα/Gal_4, PPARβ/δ/Gal_4 and PPARγ/Gal_4 receptors.

	Efficacy (%) at 10 μmol/L			EC_{50} (nmol/L)		
	PPARα	PPARβ/δ	PPARγ	PPARα	PPARβ/δ	PPARγ
4	47	NA	39	493	NA	3,270
5	48	NA	42	226	NA	5,540
6	22	NA	14	NA	NA	NA
7	1	NA	8	NA	NA	NA
8	24	NA	15	NA	NA	NA
9	11	NA	16	NA	NA	NA
13	28	NA	13	NA	NA	NA
14	121	43	11	3,255	1,475	NA
WY-14,643	100	NA	NA	4,193	NA	NA
GW501516	NA	100	NA	NA	4	NA
Rosiglitazone	NA	NA	100	NA	NA	60

Efficacy: Emax was the maximal PPAR fold-activation relative to maximum activation obtained with WY14,643 (10 μM), GW501516 (1 μM) and rosiglitazone (1 μM) corresponded to 100% in GAL4 chimeric hPPARα, hPPARβ/δ and hPPARγ system. NA: not active.

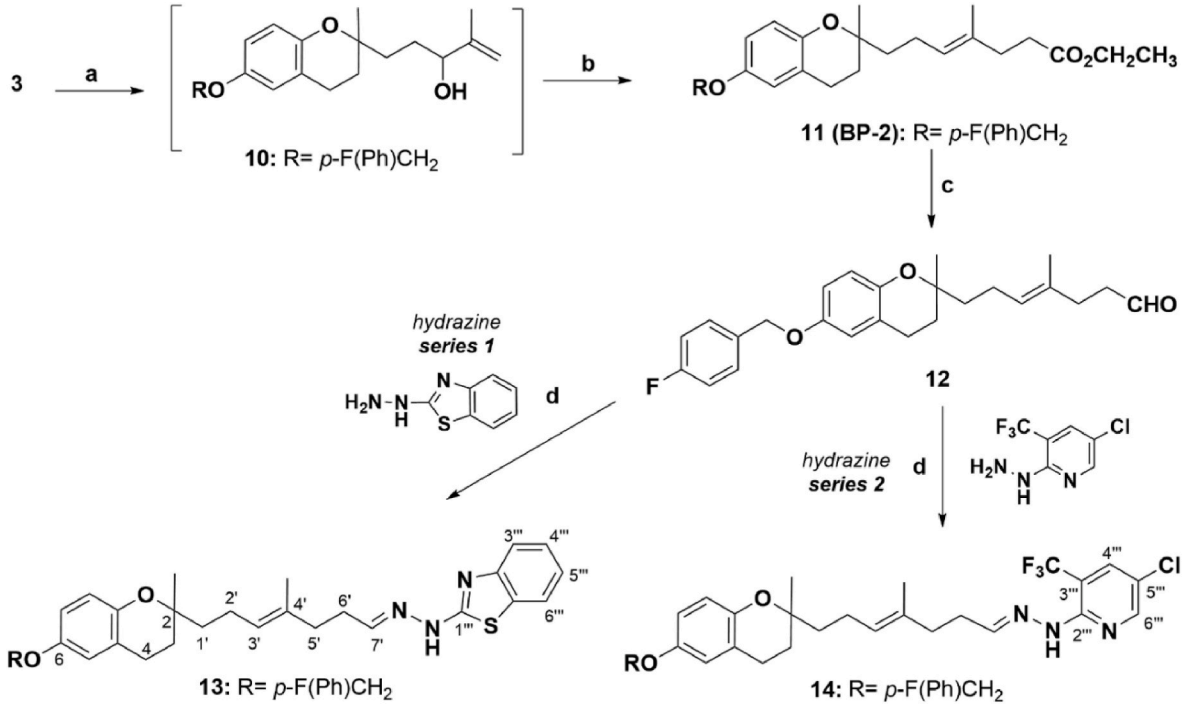

Scheme 2. Synthesis of benzopyran hydrazones with a 7-carbon length side chain. *Reagents and conditions*: (a) $CH_3C(MgBr)═CH_2$, THF, −78 °C, N_2, 3 h; (b) MeC(OEt)$_3$, isobutyric acid, 140 °C, 2 h (48%); (c) 1 M DIBAL-H in THF, CH_2Cl_2, -78 °C, 15 min (89%); (d) hydrazines: 2-hydrazinobenzothiazole or 1-[5-Cl-3-(CF_3-2-pyridyl)]$NHNH_2$, dry $(CH_2)_2Cl_2$, r.t, N_2, 1 h (70% for **13**; 60% for **14**).

1-[5-chloro-3-(trifluoromethyl)-2-pyridyl]hydrazone moiety, displayed dual hPPARα/δ activation with a full PPARα agonism. SAR studies established that: i) the free phenol group was detrimental for PPAR activation and afforded non-active analogues **8** and **9**, compared to *p*-flurobenzylbenzopyran hydrazones **4** and **5**, respectively; ii) the reduction of the imine bond of hydrazones **4** and **5** led to non-active hydrazines **6** and **7**, which indicated that the C(sp^2) = N–NH- function that contains a C═N bond conjugated with a lone pair of electrons of the amine nitrogen atom (–NH–) plays a key role in the interaction with the binding pocket of hPPARs; iii) the elongation of the isoprenyl side chain at 2-position to 7-carbons to give benzopyran **14** (*series 2*) drastically increased the activation for hPPARα, and moderately for hPPARβ/δ instead of hPPARγ moiety, but not in benzopyran **13** (*series 1*). Therefore, we have discovered novel hits (**4**, **5** and **14**), containing a hydrazone framework which exhibited dual PPARα/γ or PPARα/δ partial agonism, depending on the length of the side chain. Hydrazones (C═N^1–N^2) have been reported to possess great intrinsic hydrolytic stability due to the participation of N^2 in electron delocalization [41]. We previously demonstrated the importance of bioisosteric replacement in carboxylic function (polar head) of polycerasoidol by ester, amide and *O*-alkoxylated bioisosters to modulate hPPARα and hPPARγ interactions [20–23]. In addition, given the potential metabolic instability and toxicity associated to an acid functionality, the use of bioisosters could counter such issues and improve drug-like properties of the new PPAR agonists [42]. In this work, both benzothiazole and pyridyl groups have also shown ability to replace carboxylic moiety to activate hPPAR isoforms. Furthermore, these groups, which appear in many clinically approved drugs, have been reported to provide a good solubility range and stability in polar solvents and human plasma [43,44].

2.3. Molecular Modelling studies

At the molecular level, to understand the dual PPARα/γ agonism for hydrazones **4** and **5**, as well as the dual PPARα/δ agonism for hydrazone **14**, we carried out a combined analysis by means of a docking study and MD simulations. These studies predict how compounds **4**, **5** and **14** bind in the same region of the active site of PPARα as that reported for WY-14,643 [45,46] (Fig. 4A–C). These results can be observed in the per residue analysis, which was performed on the different ligand-receptor complexes (Fig. S1, Supporting Information). MD simulations indicate that these molecules are arranged spatially in a slightly different way. In agreement with the results obtained for WY-14643, the simulations obtained for the complexes showed the relevance of His440, Leu321 and Ser280 for ligand binding [45,46]. The other residues with significant interactions to stabilise these complexes are Cys276, Thr464, Lys358 and Ile317. In accordance with our experimental data, the interactions obtained for compounds **4** and **5** were generally weaker than those observed for WY-14,643 (Fig. S1), while the interactions obtained for hydrazone **14** were closely related to those observed for the reference compound **(**Fig. S1). With the PPARγ receptor, our simulations indicated that hydrazones **4** and **5** bound to the active site in a closely related way to that reported for rosiglitazone [47,48] (Fig. 3D and E). Indeed, hydrazones **4** and **5** interacted mainly with Cys285, Arg288, Tyr324, Leu330, Ile342, Phe366, Met364, His449 and Tyr473, although they generally displayed weaker interactions compared to rosiglitazone (Fig. S1). In contrast, the complex of hydrazone **14** with PPARδ (Fig. 4F) showed this hydrazone with a 7-carbon side chain to be spatially arranged in a similar way to reference compound GW501516 [49]. The analysis per residues of **14** (Fig. S1) showed that its interactions with PPARδ were significantly weaker to those formed by GW501516, which falls in line with our experimental results.

2.4. Anti-inflammatory effects of benzopyran hydrazones *4, 5 and 14*

In order to evaluate the anti-inflammatory effect of the dual PPARα/γ and PPARα/δ agonists on macrophages, the PMA-differentiated THP-1 cells were treated with benzopyran hydrazones **4**, **5** and **14** at 10 μM prior to the LPS stimulation. The mRNA expression and secretion of the pro-inflammatory markers, such as chemokine MCP-1 and cytokine IL-6, were determined in the LPS-stimulated THP-1 macrophages for 4 h and 24 h. The results at 4 h showed that benzopyran **4**, with a 3-carbon side chain and benzothiazole moiety, decreased the gene expression of MCP-1 and IL6 by 67% and 71%, respectively. Its pyridyl analogues **5** and **14**, respectively bearing a 3-carbon and 7-carbon side chain, showed a moderate activity. The results at 24 h revealed that benzopyran **4** inhibited the gene expression of MCP-1 and IL-6 by 71% and 93%, respectively, but also the chemo- and cytokine secretion by 85% and 79%, respectively. Its pyridyl analogue **5** moderately reduced the gene expression of MCP-1 (54%) and IL-6 (63%), and did not inhibit their secretion in the LPS-stimulated THP-1 macrophages. Finally, dual PPARδ/γ agonist **14** lowered the IL-6 gene expression levels by 88% at 24 h and reduced the secretion of both MCP-1 and IL-6 by 70–80% in the LPS-stimulated THP-1 macrophages (Fig. 5). Therefore, **4**, **5** and **14** may ameliorate the inflammation state associated with the progression of metabolic disorders.

2.5. Anti-inflammatory effects of benzopyran hydrazones *4, 5 and 14* via NF-κB

In order to investigate the intracellular signalling pathways underlying the anti-inflammatory effect of hydrazones **4**, **5** and **14**, the THP-1 cells were stimulated with LPS for 1 h in the presence or absence of compounds (10 μM, 24 h) prior to the pathway analysis. The results showed that the three hydrazones significantly blunted the TNFα-induced phosphorylation of NF-κB by 34% for **4**, 35% for **5** and 36% for **14** (Figs. 6 and 7).

2.6. Cytotoxicity study of compounds *4,5 and 15*

Apoptosis cell death was studied by an Annexin V-FITC/PI dual staining assay on THP-1 cells. None of the three compounds showed toxicity at doses 10 μM and 30 μM, and only hydrazone **5** displayed slight toxicity at the highest concentration of 100 μM (Figs. 8 and 9).

3. Conclusions

We herein efficiently prepared two series of benzopyran hydrazones and hydrazines as *polycerasoidol* analogues containing the hydrazone function in the 3-carbon or 7-carbon side chain at 2-position of the benzopyran nucleus. Benzopyran hydrazones **4** and **5** with a 3-carbon side chain, showed dual hPPARα/γ partial agonism, and hydrazone **14,** with 1-[5-chloro-3-(trifluoromethyl)-2-pyridyl]hydrazone moiety on the prenylated 7-carbon side chain, exerted dual PPARα/δ partial agonism. However, the direct reduction of hydrazones **4** and **5** effectively provided hydrazine derivatives **8** and **9**, respectively, which were inactive in any PPAR isoform. The SAR studies indicated that the side chain at the 2-postion in the benzopyran nucleus required the C═N double bond in the hydrazone function to activate the PPAR isoforms. Structurally speaking, the hydrazone function alongside the presence or absence of a prenylated moiety on the elongated side chain can modulate the activation of the PPAR isoforms. In addition, hydrazones **4**, **5** and **14** greatly attenuated inflammatory markers such as IL-6 and MCP-1, on the THP-1 cells via NF-κB activation, which are associated with obesity, type 2 diabetes and the progression of metabolic disorders. Therefore, benzopyran hydrazones emerge as novel dual PPARα/γ or dual PPARα/δ agonists with the potential for treat metabolic diseases.

4. Experimental section

4.1. Chemistry methods

High-resolution electrospray ionization mass spectrometry (HRMS

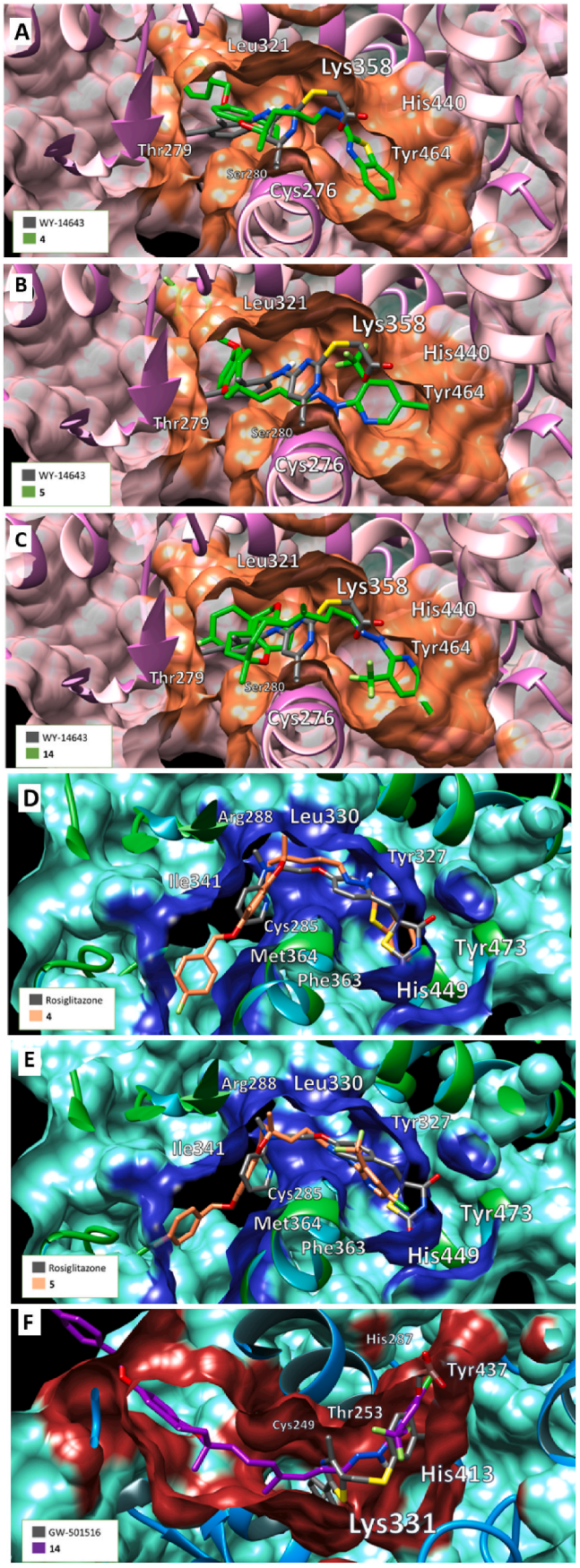

(caption on next column)

Fig. 4. Spatial view of interactions for WY-14,643, rosiglitazone or GW501516, and active benzopyran hydrazones bonded in the binding pocket of PPARα, PPARγ or PPARδ by docking experiments. Spatial view of (A) WY-14,643 (grey) and **4** (green)/PPARα interaction, (B) WY-14,643 (grey) and **5** (green)/PPARα, (C) WY-14,643 (grey) and **14** (green)/PPARα, (D) rosiglitazone (grey) and **4** (pink)/PPARγ interaction, (E) rosiglitazone (grey) and hydrazone **5** (purple)/PPARγ, (F) GW501516 (grey) and **14** (pink)/PPARδ. The orange, blue or burgundy zone represent the binding site for PPARα, PPARγ or PPARδ, respectively, and the rest is shown in pink color or light green. The names of the residues stabilizing the complex are remarked in the figure.

(ESI)) was performed on a TripleTOF™ 5600 LC/MS/MS System (AB SCIEX) (Toronto, Canada). Liquid chromatography-mass spectrometry detection was performed on a liquid chromatography UHPLC apparatus (Shimadzu, LCMS-8040) coupled to a tandem mass spectrometry (MS/MS) triple quadrupole equipped with electrospray ionization (ESI) ion source (Shimadzu, Kyoto, Japan). ^{1}H and ^{13}C NMR spectra were recorded on a Bruker AC-300 or AC-500 (Bruker Instruments, Kennewick, WA). The assignments in ^{1}H and ^{13}C NMR were made by COSY 45, HSQC and HMBC correlations. Chemical shifts (δ) are reported in ppm relative to an internal deuterated solvent reference, with multiplicities indicated as s (singlet), br (broad singlet), d (doublet), t (triplet), q (quartet) m (multiplet) or dd (double doblet). All reactions were monitored by analytical TLC with silica gel 60 F254 (Merck 5554). All reactions were monitored by analytical thin-layer chromatography with silica gel 60 F_{254} (Merck 5554; Merck Group, Darmstadt, Germany). Residues were purified by silica gel column chromatography (40–63 μm, Merck Group). Solvents and reagents were purchased from the commercial sources Scharlab S.L. (Barcelona, Spain) and Sigma-Aldrich (St. Louis, MO), respectively, and used without further purification unless otherwise noted. Dry and freshly distilled solvents were used in those reactions performed under N_2. Quoted yields are of purified material. Final compounds were purified to ≥95% as assessed by ^{1}H NMR and LC-MS/MS analysis.

4.2. Ethyl 3-(6-(p-fluorobenzyloxy)-2-methyldihydrobenzopyran-2yl) propanoate (2)

Ethyl 3-(6-hydroxy-2-methylbenzopyran-4-one-2yl)propanoate (1.2 g, 4.32 mmol) was dissolved in a mixture of AcOH-H_2O (2:1, v/v) (14 mL). Then, Zn dust (5.07 g, 76.45 mmol) followed by concentrated HCl (9 mL) was added slowly in small portions for 30 min. After stirring for an additional 1 h at room temperature, water (15 mL) was added and the mixture was extracted with AcOEt (3 × 15 mL). The organic layers were combined, dried over anhydrous Na_2SO_4, and evaporated under reduced pressure. The residue was purified by column chromatography (hexane/EtOAc, 85:15) to yield the ethyl 3-(6-hydroxy-2-methyldihydrobenzopyran-2yl)propanoate (**1**, 0.66 g, 2.50 mmol, 58%) as a colorless oil [24]. A solution of benzopyran ester **1** (500 g, 1.89 mmol), *p*-fluorobenzyl chloride (0.3 mL, 2.46 mmol), anhydrous K_2CO_3 (0.4 g, 2.83 mmol) in absolute EtOH (20 mL) was refluxed under N_2 for 4 h. The mixture was evaporated, water was added (20 mL) and the mixture was extracted with dichloromethane (3 × 15 mL). The organic layers were combined, washed with 1 M HCl and brine, dried over anhydrous Na_2SO_4, and evaporated under reduced pressure. The residue was purified by column chromatography (hexane/EtOAc, 90:10) to yield the O-protected benzopyran ester (**2**) (556 mg, 1.49 mmol, 79%) as a colorless oil. ^{1}H NMR (300 MHz, $CDCl_3$) δ 7.41–7.36 (m, 2H, CH-2″, CH-6″), 7.09–7.03 (m, 2H, CH-3″, CH-5″), 6.72–6.67 (m, 3H, CH-5, CH-7, CH-8), 4.94 (s, 2H, OCH_2Ph-*p*-F), 4.13 (q, J = 7.1 Hz, 2H, $CO_2CH_2CH_3$), 2.76 (t, J = 6.7 Hz, 2H, CH_2-4), 2.48 (t, J = 7.7 Hz, 2H, CH_2-2′), 2.0–1.75 (m, 4H, CH_2-3, CH_2-1′), 1.24 (t, J = 7.2 Hz, 3H, $CO_2CH_2CH_3$), 1.23 (s, 3H, CH_3-2); ^{13}C NMR (75 MHz, $CDCl_3$) δ 173.6 ($COOCH_2CH_3$), 162.3 (d, J_{CF} =244 Hz, C-4″), 152.0 (C-6), 147.9 (C-8a), 133.1 (d, J_{CF} = 3 Hz, C-1″), 129.1 (d, J_{CF} = 8 Hz, CH-2″, CH-6″), 121.4 (C-4a), 117.7 (CH-5), 115.2 (d, J_{CF} = 25 Hz, CH-3″, CH-5″), 115.1 (CH-7), 114.4 (CH-8), 74.6

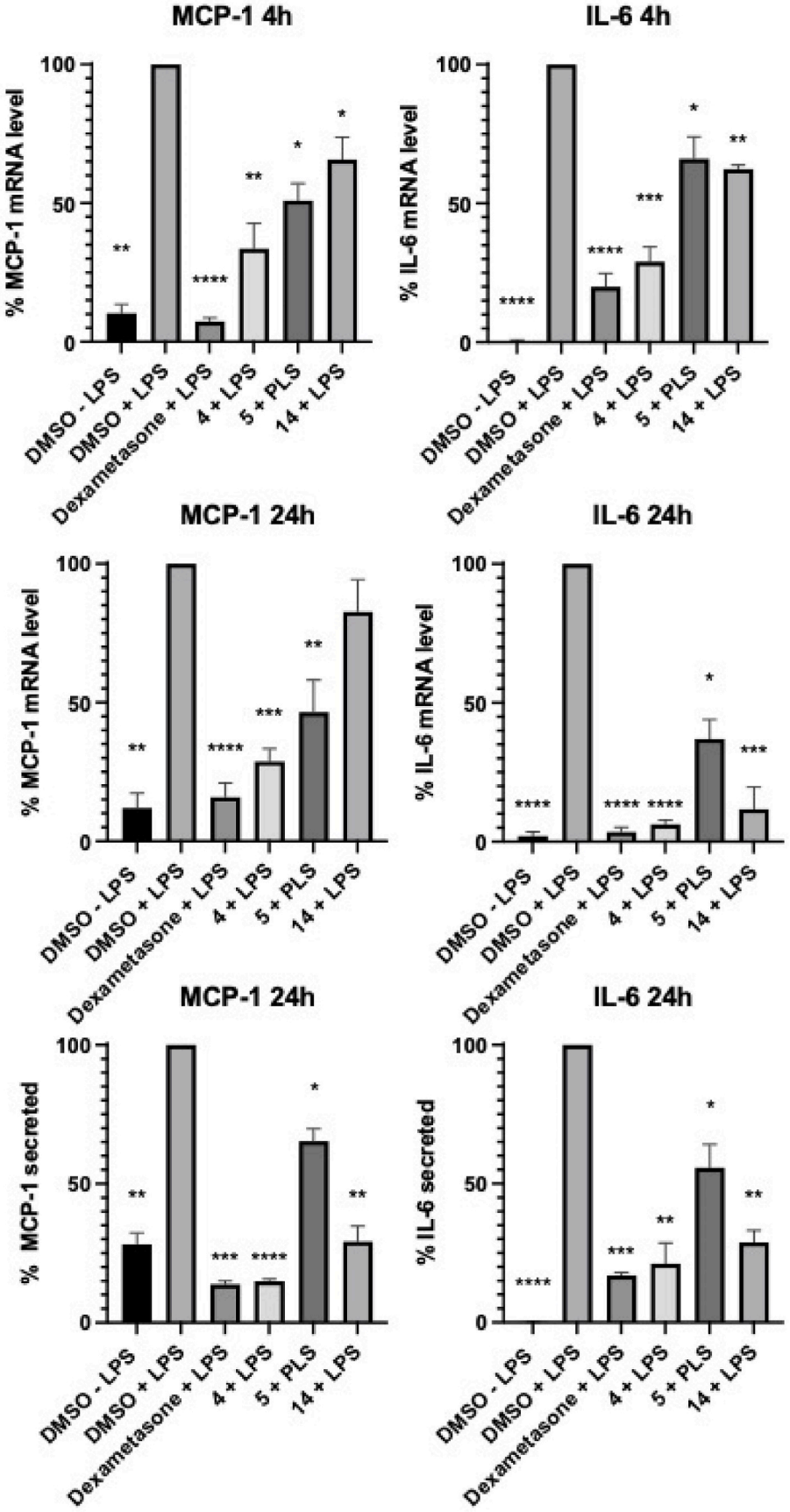

(caption on next page)

Fig. 5. Anti-inflammatory effects of hydrazones **4**, **5**, **14**, and dexamethasone by inhibition of pro-inflammatory cytokine IL-6 and chemokine MCP-1 production in LPS-induced THP-1 cells. THP-1 cells were pretreated with benzopyran hydrazones **4**, **5** and **14** (10 μM) or dexamethasone (Dexa) (positive control at 10^{-8} μM) for 1 h before stimulation with LPS (100 ng/mL) for 4 h and 24 h. The levels of IL-6 and MCP-1 were measured using qPCR (A, B, C, D) or ELISA (E, F). The data are expressed as % of LPS stimulated condition and presented as means ± SD of three independent experiments performed in triplicate. *P < 0.05, **P < 0.01, ***P < 0.001, ****P < 0.0001 vs. LPS-induced group.

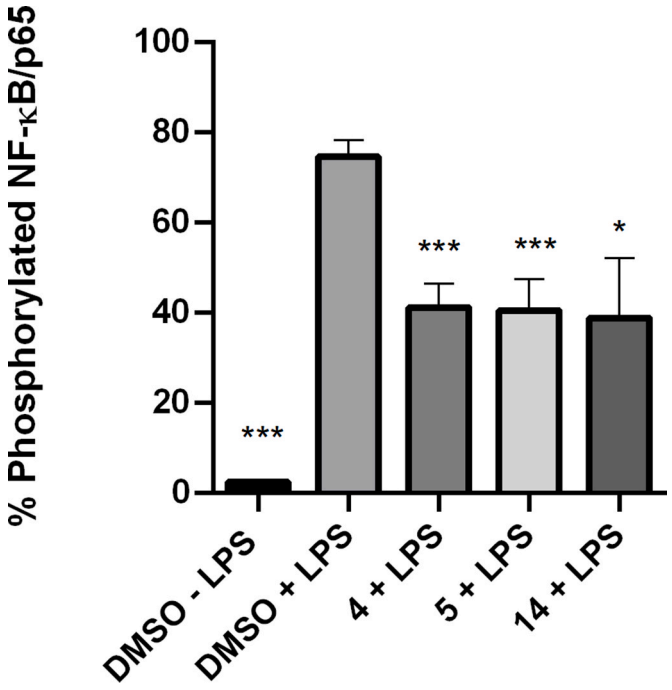

Fig. 6. Phosphorylated NF- κB/p65% of hydrazones **4**, **5**, **14** at 10 μM. on the THP-1 cells. The data are presented as means ± SD of three independent experiments performed in triplicate. *P < 0.05, ***P < 0.001 vs. LPS-induced group.

(C-2), 69.9 (O*C*H_2Ph-*p*-F), 60.3 ($CO_2CH_2CH_3$), 34.3 (CH_2-1′), 31.0 (CH_2-3), 28.7 (CH_2-2′), 23.6 (CH_3-2), 22.2 (CH_2-4), 14.1 ($CO_2CH_2CH_3$); HREIMS *m/z* calcd for $C_{22}H_{25}O_4F$ [M]+ 372.1737, found: 372.1730.

4.3. 3-(6-((p-Fluorobenzyl)oxy)-2-methyldihydrobenzopyran-2-yl) propanal (3)

A solution of **2** (250 mg, 0.67 mmol) in anhydrous dichloromethane (10 mL) at −78 °C under N_2 atmosphere was stirred for 10 min. To this solution was added dropwise 4.4 mL of 1.0 M DIBAL-H solution in THF. After 15 min, the mixture was quenched by addition of 5 mL of MeOH and 10 mL of halfsat aqueous NH_4Cl solution. The reaction mixture was stirred for additional 10 min at room temperature and concentrated in vacuo. Then, water was added and extracted with EtOAc (3 x 15 mL). The combined organic layers were washed with water, dried over anhydrous Na_2SO_4 and evaporated to dryness. The residue was purified by silica gel column chromatography (hexane/EtOAc, 90:10) to afford the corresponding aldehyde **3** (203 mg, 0.62 mmol, 92%) as a colorless oil. ^{1}H NMR (300 MHz, $CDCl_3$) δ 9.78 (t, J = 1.6 Hz, 1H, CHO), 7.39–7.37 (m, 2H, CH-2″, CH-6″), 7.08–7.04 (m, 2H, CH-3″, CH-5″), 6.74–6.67 (m, 3H, CH-5, CH-7, CH-8), 4.94 (s, 2H, O*CH*$_2$Ph-*p*-F), 2.77–2.74 (m, 2H, CH_2-4), 2.62–2.59 (m, 2H, CH_2-2′), 2.03–1.75 (m, 4H, CH_2-3, CH_2-1′), 1.26 (s, 3H, CH_3-2); ^{13}C NMR (75 MHz, $CDCl_3$) δ 202.2 (CHO), 162.4 (d, J_{CF} = 244 Hz, C-4″), 152.1 (C-6), 147.7 (C-8a), 133.1 (d, J_{CF} = 3 Hz, C-1″), 129.3 (d, J_{CF} = 8 Hz, CH-2″, CH-6″), 121.4 (C-4a), 117.7 (CH-5), 115.2 (d, J_{CF} = 25 Hz, CH-3″, CH-5″), 115.2 (CH-7), 114.5 (CH-8), 74.6 (C-2), 69.9 (O*C*H_2Ph-*p*-F), 38.4 (CH_2-2′), 31.8 (CH_2-1′), 31.2 (CH_2-3), 23.7 (CH_3-2), 22.3 (CH_2-4); HRMS (ESI) *m/z* calcd for $C_{20}H_{21}O_3F$ [M+H] + 329.1547, found: 329.1552.

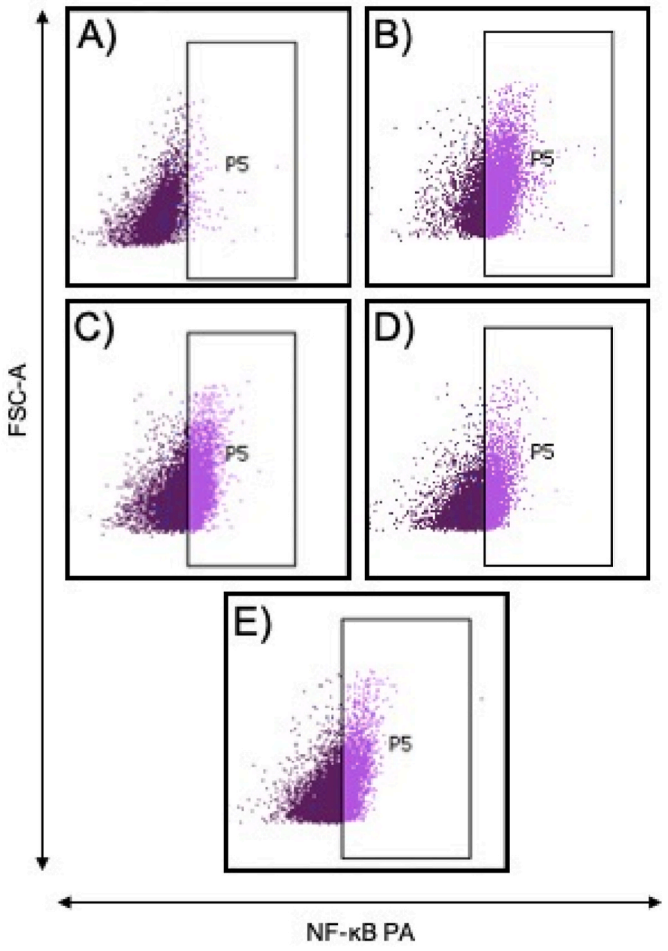

Fig. 7. Representative images of one of the flow cytometry analyses for **4**, **5** and **14** at 10 μM of activated NF-κB on the THP-1 macrophages. A) DMSO, B) **4,** C) **5,** D) **14**.

4.4. General procedure for synthesis of hydrazone benzopyrans (4, 5)

A mixture of aldehyde **3** (58.1 mg, 0.18 mmol) and 2-hydrazinobenzothiazole (48.6 mg, 0.294 mmol) or 1-[5-chloro-3-(trifluoromethyl)-2-pyridyl]hydrazine (62.2 mg, 0.29 mmol) in anhydrous dichloroethane (3 mL) was stirred for 1 h under N_2. The resulting mixture was basified with 5% aq NH_3 and then, water was added and extracted EtOAc (3 x 5 mL). The combined organic layers were dried over anhydrous Na_2SO_4 and evaporated to dryness. The residues obtained were purified by silica gel column chromatography (hexane/EtOAc, 80:20) to afford hydrazone **4** (68.6 mg, 0.14 mmol, 80 %) as a reddish oil or **5** (82.3 mg, 0.16 mmol, 89 %) as a yellowish oil.

4.4.1. 2-(2-(3-(6-((p-Fluorobenzyl)oxy)-2-methylbenzodihydropyran-2-yl)propylidene) hydrazineyl)benzo[d]thiazole (4)

^{1}H NMR (300 MHz, $CDCl_3$) δ 8.96 (1H, brs, NH), 7.62 (dd, J= 7.8 Hz, 1.3 Hz, 1H, CH-3‴), 7.42–7.35 (m, 3H, CH-2″, CH-6″, CH-6‴), 7.29–7.25 (m, 2H, CH-4‴, CH-3′), 7.11–7.03 (m, 3H, CH-3″, CH-5″, CH-5‴), 6.72–6.67 (m, 3H, CH-5, CH-7, CH-8), 4.92 (s, 2H, O*CH*$_2$Ph-*p*-F), 2.77–2.75 (m, 2H, CH_2-4), 2.36–2.31 (m, 2H, CH_2-2′), 1.78–1.74 (m, 4H,

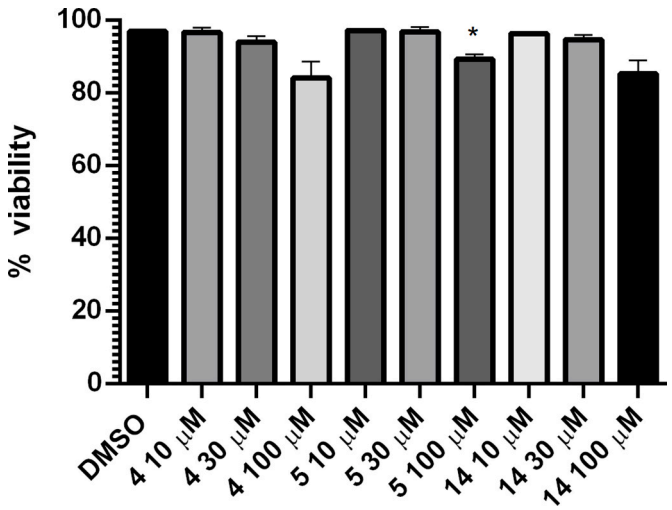

Fig. 8. Cytotoxic effects of hydrazones **4**, **5**, **14** on the THP-1 cells. The data are presented as means ± SD of three independent experiments performed in triplicate. *P < 0.05 vs. LPS-induced group.

CH_2-1′, CH_2-3), 1.27 (s, 3H, CH_3-2); ^{13}C NMR (75 MHz, $CDCl_3$): δ 168.9 (C-1‴), 162.4 (d, J_{CF} = 244 Hz, C-4″), 152.0 (C-6), 149.9 (C-2a‴), 147.9 (CH-3′, C-8a), 133.1 (d, J_{CF} = 3 Hz, C-1″), 129.8 (C-6a‴), 129.2 (d, J_{CF} = 8 Hz, CH-2″, CH-6″), 125.9 (CH-4‴), 121.7 (CH-5‴), 121.5 (C-4a), 121.3 (CH-3‴), 117.7 (CH-5), 117.6 (CH-6‴), 115.3 (d, J_{CF} = 21 Hz, CH-3″, CH-5″), 115.2 (CH-7), 114.4 (CH-8), 75.1 (C-2), 69.9 (OCH_2Ph-*p*-F), 35.7 (CH_2-1′), 31.1 (CH_2-3), 26.7 (CH_2-2′), 23.9 (CH_3-2), 22.3 (CH_2-4); HRMS (ESI) *m/z* calcd for $C_{27}H_{26}FN_3O_2S$ [M+H] + 476.1803, found: 476.1808.

4.4.2. 5-Chloro-2-(2-(3-(6-((p-fluorobenzyl)oxy)-2-methylbenzodihydropyran-2-yl) propylidene)hydrazineyl)-3-(trifluoromethyl)pyridine (5)

^{1}H NMR (300 MHz, $CDCl_3$) δ 8.47–8.44 (m, 1H, CH-6‴), 8.36–8.33 (brs, 1H, NH), 7.72 (d, *J*= 2 Hz, 1H, CH-4‴), 7.42–7.36 (m, 3H, CH-2″, CH-6″, CH-3′), 7.07–7.01 (m, 2H, CH-3″, CH-5″), 6.75–6.64 (m, 3H, CH-5, CH-7, CH-8), 4.92 (s, 2H, OCH_2Ph-*p*-F), 2.78–2.71 (m, 2H, CH_2-4), 2.66–2.57 (m, 2H, CH_2-2′), 1.96–1.72 (m, 4H, CH_2-3, CH_2-1′), 1.29 (s, 3H, CH_3-2); ^{13}C NMR (75 MHz, $CDCl_3$): δ 162.4 (d, J_{CF} = 244 Hz, C-4″), 152.3 (q, J_{CF} = 4 Hz, C-2‴), 152.0 (C-6), 149.6 (CH-3′), 147.8 (C-8a), 144.5 (CH-6‴), 133.8 (q, J_{CF} = 3 Hz, CH-4‴), 133.1 (d, J_{CF} = 3 Hz, C-1″), 129.2 (d, J_{CF} = 8 Hz, CH-2″, CH-6″), 123.2 (q, J_{CF}= 270 Hz, CF_3), 121.6 (C-4a), 118.5 (q, J_{CF} = 33 Hz, C-3‴), 117.8 (CH-5), 115.3 (d, J_{CF} = 21 Hz, CH-3″, CH-5″), 114.6 (CH-7), 114.3 (C-5‴), 113.8 (CH-8), 75.2 (C-2), 70.0 (OCH_2Ph-*p*-F), 36.4 (CH_2-1′), 31.2 (CH_2-3), 26.9 (CH_2-2′), 23.9 (CH_3-2), 22.3 (CH_2-4); HRMS (ESI) *m/z* calcd for $C_{26}H_{24}ClF_4N_3O_2$ [M+H] + 522.1566, found: 522.1567.

4.5. General procedure for O-deprotection to prepare compounds 6 and 7

A solution of compound **4** (30 mg, 0.063 mmol) or **5** (33 mg, 0.063 mmol) in anhydrous dichloromethane (1 mL) was added BBr_3 (0.25 mL, 0.25 mmol) at −78 °C, and stirred for 15 min under N_2 atmosphere. Then, the reaction mixture was stirred under N_2 and at room temperature for an additional 45 min. The resulting mixture was basified with 5% NH_3 and then, water was added and extracted with EtOAc (3 x 5 mL). The combined organic layers were dried over anhydrous Na_2SO_4 and evaporated to dryness. The residue obtained was purified by silica gel column chromatography (CH_2Cl_2/MeOH, 98:2) to afford compound **6** (21 mg, 0.06 mmol, 91 %) as a greenish oil and compound **7** (24 mg,0.06 mmol, 92 %) as a yellowish oil, respectively.

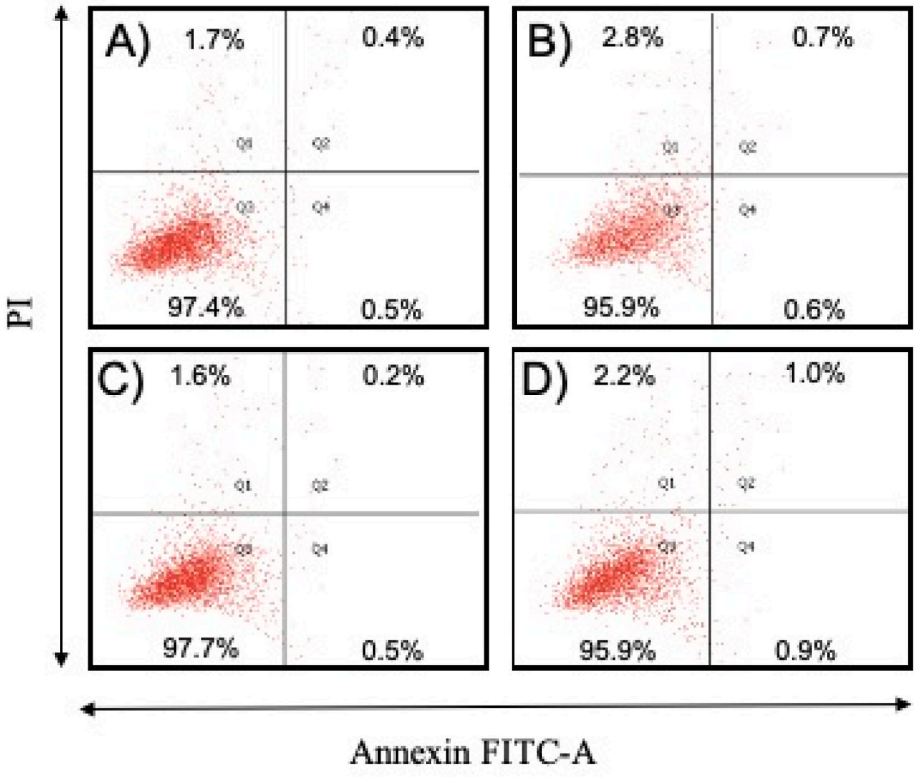

Fig. 9. Representative images of one of the apoptosis/necrosis analyses for **4**, **5** and **14** at 30 μM on the THP-1 macrophages. A) DMSO, B) **4**, C) **5,** D) **14**.

4.5.1. 2-(3-(2-(Benzo[d]thiazol-2-yl)hydrazineylidene)propyl)-2-methylbenzodihydropyran-6-ol (6)

^{1}H NMR (300 MHz, $CDCl_3$ + 1 drop CD_3OD) δ 7.59 (dd, J= 7.8 Hz, 1.3 Hz, 1H, CH-3‴), 7.45–7.42 (m, 1H, CH-6‴), 7.37–7.23 (m, 2H, CH-4‴, CH-3′), 7.16–7.06 (m, 1H, CH-5‴), 6.67–6.43 (m, 3H, CH-5, CH-7, CH-8), 2.75–2.65 (m, 2H, CH_2-4), 2.51–2.37 (m, 2H, CH_2-2′), 1.91–1.64 (m, 4H, CH_2-1′, CH_2-3), 1.27 (s, 3H, CH_3-2); ^{13}C NMR (75 MHz, $CDCl_3$ + 1 drop CD_3OD): δ 168.0 (C-1‴), 149.9 (C-2a‴), 149.4 (C-6), 147.7 (C-8a), 146.9 (CH-3′), 128.9 (C-6a‴), 126.3 (CH-4‴), 122.4 (CH-5‴), 121.6 (C-4a), 121.3 (CH-3‴), 117.7 (CH-5), 117.4 (CH-6‴), 115.3 (CH-7), 114.5 (CH-8), 74.9 (C-2), 35.5 (CH_2-1′), 31.2 (CH_2-3), 26.9 (CH_2-2′), 23.9 (CH_3-2), 22.1 (CH_2-4); HRMS (ESI) *m/z* calcd for $C_{20}H_{22}N_3O_2S$ [M+H] + 368.1433, found: 368.1417.

4.5.2. 2-(3-(2-(5-chloro-3-(trifluoromethyl)pyridin-2-yl) hydrazineylidene)propyl)-2-methylbenzodihydropyran-6-ol (7)

^{1}H NMR (300 MHz, $CDCl_3$ + 1 drop CD_3OD) δ 8.39–8.38 (m, 1H, CH-6‴), 7.90 (brs, 1H, NH), 7.74–7.73 (m, 1H, CH-4‴), 7.31 (t, J= 3 Hz, 1H, CH-3′), 6.64–6.52 (m, 3H, CH-5, CH-7, CH-8), 2.77–2.69 (m, 2H, CH_2-4), 2.62–2.55 (m, 2H, CH_2-2′), 1.92–1.72 (m, 4H, CH_2-3, CH_2-1′), 1.28 (s, 3H, CH_3-2); ^{13}C NMR (75 MHz, $CDCl_3$ + 1 drop CD_3OD) δ 150.8 (CH-6‴), 149.6 (q, J_{CF}= 4 Hz, C-2‴), 148.8 (C-8a, C-6), 147.4 (CH-3′), 135.4 (q, J_{CF}= 4 Hz, CH-4‴), 123.2 (q, J_{CF}= 270 Hz, CF_3), 121.7 (C-4a), 118.5 (q, J_{CF} = 33 Hz, C-3‴), 117.7 (CH-5), 115.4 (CH-7), 114.6 (CH-8), 108.8 (C-5‴), 75.0 (C-2), 36.2 (CH_2-1′), 31.1 (CH_2-3), 26.8 (CH_2-2′), 23.9 (CH_3-2), 22.1 (CH_2-4); HRMS (ESI) *m/z* calcd for $C_{19}H_{17}ClF_3N_3O_2$ [M+H] + 412.1034, found: 412.1028.

4.6. General procedure for synthesis of hydrazine benzopyrans (8, 9)

A solution of compound **4** (37.9 mg, 0.08 mmol) or **5** (41.4 mg, 0.08 mmol) in anhydrous MeOH (4 mL) was added $NaBH_4CN$ (15 mg, 0.238 mmol) and two drops of BF_3OEt. The reaction was refluxed for 1 h under N_2 atmosphere. The resulting mixture was basified with 5% NH_3 and then, water was added and extracted ethyl acetate (3 x 5 mL). The combined organic layers were washed with water, dried over anhydrous Na_2SO_4 and evaporated to dryness. The residue obtained was purified by silica gel column chromatography (hexane/EtOAc, 60:40 or hexane/EtOAc, 85:15) to afford compound **8** (37 mg, 0.08 mmol, 96%) as a bluish grey oil and compound **9** (31 mg, 0.06 mmol, 75%) as a reddish yellow oil.

4.6.1. 2-(2-(3-(6-((p-Fluorobenzyl)oxy)-2-methylbenzodihydropyran-2-yl)propyl)hydrazineyl) benzo[d]thiazole (8)

^{1}H NMR (300 MHz, $CDCl_3$) δ 7.64 (dd, J= 8 Hz, 1.2 Hz, 1H, CH-3‴), 7.48 (dd, J= 8 Hz, 1.2 Hz, 1H, CH-6‴), 7.43–7.37 (m, 2H, CH-2″, CH-6″), 7.29 (td, J= 8 Hz, 1.2 Hz, 1H, CH-4‴), 7.13–7.03 (m, 3H, CH-3″, CH-5″, CH-5‴), 6.75–6.65 (m, 3H, CH-5, CH-7, CH-8), 4.94 (s, 2H, OCH_2Ph-*p*-F), 3.07–2.92 (m, 2H, CH_2-3′), 2.71 (t, J= 7 Hz, 2H, CH_2-4), 1.82–1.61 (m, 6H, CH_2-1′, CH_2-2′, CH_2-3), 1.24 (s, 3H, CH_3-2); ^{13}C NMR (75 MHz, $CDCl_3$): δ 174.0 (C-1‴), 162.3 (d, J_{CF} = 244 Hz, C-4″), 152.3 (C-6), 151.9 (C-2a‴), 148.0 (C-8a), 133.1 (d, J_{CF} = 3 Hz, C-1″), 130.6 (C-6a‴), 129.2 (d, J_{CF} = 8 Hz, CH-2″, CH-6″), 125.6 (CH-4‴), 121.6 (C-4a), 121.2 (CH-3‴), 121.0 (CH-5‴), 118.3 (CH-6‴), 117.7 (CH-5), 115.3 (d, J_{CF} = 21 Hz, CH-3″, CH-5″), 115.1 (CH-7), 114.3 (CH-8), 75.4 (C-2), 69.9 (OCH_2Ph-*p*-F), 52.6 (CH_2-3′), 36.9 (CH_2-1′), 30.8 (CH_2-3), 23.8 (CH_3-2), 22.3 (CH_2-2′), 22.0 (CH_2-4); HRMS (ESI) *m/z* calcd for $C_{27}H_{26}FN_3O_2S$ [M+H] + 476.1803, found: 476.1802.

4.6.2. 5-Chloro-2-(2-(3-(6-((p-fluorobenzyl)oxy)-2-methylbenzodihydropyran-2-yl)propyl) hydrazineyl)-3-(trifluoromethyl) pyridine (9)

^{1}H NMR (300 MHz, $CDCl_3$) δ 8.32–8.28 (m, 1H, CH-6‴), 7.72 (d, J= 2.0 Hz, 1H, CH-4‴), 7.42–7.33 (m, 2H, CH-2″, CH-6″), 7.11–7.01 (m, 2H, CH-3″, CH-5″), 6.77–6.61 (m, 3H, CH-5, CH-7, CH-8), 4.94 (s, 2H, OCH_2Ph-*p*-F), 2.98–2.89 (m, 2H, CH_2-3′), 2.80–2.71 (m, 2H, CH_2-4), 1.88–1.61 (m, 6H, CH_2-3, CH_2-1′, CH_2-2′), 1.27 (s, 3H, CH_3-2); ^{13}C NMR (75 MHz, $CDCl_3$): δ 162.4 (d, J_{CF} = 244 Hz, C-4″), 153.3 (q, J_{CF} = 4 Hz, C-2‴), 152.0 (C-6), 149.6 (CH-6‴), 148.2 (C-8a), 135.2 (q, J_{CF} = 4 Hz, CH-4‴), 133.3 (d, J_{CF} = 3 Hz, C-1″), 129.2 (d, J_{CF} = 8 Hz, CH-2″, CH-6″), 123.2 (q, J_{CF} = 270 Hz, CF_3), 121.7 (C-4a), 119.9 (q, J_{CF} = 33 Hz, C-3‴), 117.8 (CH-5), 115.4 (d, J_{CF} = 21 Hz, CH-3″, CH-5″), 115.2 (CH-7), 114.4 (CH-8), 109.3 (C-5‴), 75.6 (C-2), 70.0 (OCH_2Ph-*p*-F), 51.7 (CH_2-3′), 36.9 (CH_2-1′), 31.0 (CH_2-3), 24.0 (CH_2-2′), 22.4 (CH_3-2), 22.0 (CH_2-4); HRMS (ESI) *m/z* calcd for $C_{26}H_{27}ClF_4N_3O_2$ [M + H] + 524.1728, found: 524.1683.

4.7. General procedure for the synthesis of hydrazone benzopyrans (13, 14)

A solution of compound aldehyde (**3**) (130 mg, 0.40 mmol) in anhydrous THF (5 mL) was stirred at −78 °C under N_2 for 15 min and treated with 0.5 M isopropenylmagnesium bromide solution (4.8 mL, 1.35 mmol). The mixture was stirred at −78 °C for 3 h. The resulting mixture reaction was quenched by the addition of a half-saturated aqueous NH_4Cl solution. The reaction was stirred for 15 min at room temperature. Subsequently, water was added, and the mixture was extracted with ethyl acetate (3 × 15 mL). The combined organic layers were washed with brine, dried over anhydrous Na_2SO_4 and evaporated to dryness under reduced pressure. The residue obtained (162 mg) was treated without further purification with 10 mL of triethylorthoacetate and a catalytic amount of isobutyric acid (3 drops). The mixture was stirred at 140 °C for 2 h. After cooling, the mixture was concentrated under reduced pressure to remove the excess triethylorthoacetate. Then, water was added and extracted with dichloromethane (3 × 15 mL), dried over anhydrous Na_2SO_4 and concentrated under reduced pressure. The residue was purified by silica gel column chromatography (hexane/EtOAc, 98:2) to yield benzopyran ester **11** (84 mg, 0.2 mmol, 48 %) as a white solid.

4.7.1. Ethyl 7-(6-((p-fluorobenzyl)oxy)-2-methyldihydrobenzopyran-2-yl)-4-methylhept-4-enoate (11)

^{1}HNMR (500 MHz, $CDCl_3$) δ 7.41–7.36 (m, 2H, CH-2″, CH-6″), 7.09–7.06 (m, 2H, CH-3″, CH-5″), 6.72–6.66 (m, 3H, CH-5, CH-7, CH-8), 5.14 (t, J= 7.0 Hz, 1H, CH-3′), 4.94 (s, 2H, OCH_2Ph-*p*-F), 4.11 (q, J= 7.4 Hz, 2H, $CO_2CH_2CH_3$), 2.72 (t, J = 6.8, 2H, CH_2-4), 2.41–2.35 (m, 2H, CH_2-6′), 2.29–2.27 (m, 2H, CH_2-5′), 2.09–2.05 (m, 2H, CH_2-2′), 1.84–1.72 (m, 2H, CH_2-3), 1.66–1.60 (m, 2H, CH_2-1′), 1.60 (s, 3H, CH_3-4′), 1.27 (s, 3H, CH_3-2), 1.23 (t, J= 7.3 Hz, 3H, $CO_2CH_2CH_3$); ^{13}C NMR (125 MHz, $CDCl_3$) δ 173.4 (CO), 162.4 (d, J_{CF} = 244 Hz, C-4″), 151.9 (C-6), 148.2 (C-8a), 133.5 (C-4′), 133.3 (d, J_{CF} = 3 Hz, C-1″), 129.2 (d, J_{CF} = 8.3 Hz, CH-2″, CH-6″), 124.9 (C-3′), 121.7 (C-4a), 117.8 (CH-5), 115.3 (d, J_{CF} = 24.8 Hz, CH-3″, CH-5″), 115.2 (CH-7), 114.4 (CH-8), 75.6 (C-2), 70.1 (OCH_2Ph-*p*-F), 60.2 ($CO_2CH_2CH_3$), 39.2 (CH_2-6′), 34.6 (CH_2-1′), 33.2 (CH_2-5′), 30.9 (CH_2-3), 24.1 (CH_3-2), 22.4 (CH_2-2′), 22.2 (CH_2-4), 15.8 (CH_3-4′), 14.2 ($CO_2CH_2CH_3$); HREIMS *m/z* calcd for $C_{27}H_{33}FO_4$ $[M]^+$ 441.2436, found: 441.2441.

4.7.2. 7-(6-((p-Fluorobenzyl)oxy)-2-methyldihydrobenzopyran-2-yl)-4-methylhept-4-enal (12)

The title compound was prepared from benzopyran ester **11** (80 mg, 0.18 mmol) following the general procedure for the synthesis of aldehyde **3** to afford compound **12** (63 mg, 0.16 mmol, 89%) as a colorless oil. ^{1}H NMR (300 MHz, $CDCl_3$) δ 9.74 (t, J= 2 Hz, 1H, CHO), 7.42–7.36 (m, 2H, CH-2″, CH-6″), 7.09–7.03 (m, 2H, CH-3″, CH-5″), 6.73–6.67 (m, 3H, CH-5, CH-7, CH-8), 5.14 (t, J= 7 Hz, 1H, CH-3′), 4.94 (s, 2H, OCH_2Ph-*p*-F), 2.74 (t, J = 7 Hz, 2H, CH_2-4), 2.50–2.47 (m, 2H, CH_2-6′), 2.33–2.30 (m, 2H, CH_2-5′), 2.15–2.08 (m, 2H, CH_2-2′), 1.86–1.73 (m, 2H, CH_2-3), 1.71–1.54 (m, 5H, CH_2-1′, CH_3-4′), 1.27 (s, 3H, CH_3-2); ^{13}C NMR (75 MHz, $CDCl_3$) δ 202.6 (CHO), 162.4 (d, J_{CF} = 244 Hz, C-4″), 151.9 (C-6), 148.2 (C-8a), 133.4 (C-4′), 133.3 (d, J_{CF} = 3 Hz, C-1″), 129.2 (d, J_{CF} = 8 Hz, CH-2″, CH-6″), 124.9 (C-3′), 121.7 (C-4a), 117.8 (CH-5),

115.3 (d, J_{CF} = 25 Hz, CH-3″, CH-5″), 115.2 (CH-7) 114.4 (CH-8), 75.6 (C-2), 70.1 (OCH_2Ph-*p*-F), 42.1 (CH_2-6′), 39.2 (CH_2-1′), 31.8 (CH_2-5′), 31.0 (CH_2-3), 24.1 (CH_3-2), 22.4 (CH_2-2′), 22.2 (CH_2-4), 16.0 (CH_3-4′); EIMS *m/z (%)* 396.50 $[M]^+$.

4.7.3. 2-(2-(7-(6-((p-Fluorobenzyl)oxy)-2-methylbenzodihydropyran-2-yl)-4-methylhept-4-en-1-ylidene)hydrazineyl)benzo[d]thiazole (13)

The title compound was prepared from aldehyde **12** (26.50 mg, 0.07 mmol) and 2-hydrazinobenzothiazole (18.4 mg, 0.11 mmol) following the general procedure for the synthesis of compound **4**. The residue obtained was purified by silica gel column chromatography (CH_2Cl_2/MeOH, 98:2) to afford compound **13** (26.5 mg, 69.5%) as a reddish oil. ^{1}H NMR (300 MHz, $CDCl_3$) δ 7.64 (dd, *J*= 8 Hz, 1.2 Hz, 1H, CH-3‴), 7.45 (dd, *J*= 8 Hz, 1.2 Hz, 1H, CH-6‴), 7.42–7.35 (m, 2H, CH-2″, CH-6″), 7.34–7.24 (m, 2H, CH-7′, CH-4‴), 7.16–7.01 (m, 3H, CH-5‴, CH-3″, CH-5″), 6.74–6.63 (m, 3H, CH-5, CH-7, CH-8), 5.22–5.08 (m, 1H, CH-3′), 4.93 (s, 2H, OCH_2Ph-*p*-F), 2.70 (t, 2H, *J*= 7.0 Hz, CH_2-4), 2.42–2.38 (m, 2H, CH_2-5′), 2.21 (t, 2H, *J*= 7.7 Hz, CH_2-6′), 2.17–2.05 (m, 2H, CH_2-2′), 1.89–1.67 (m, 2H, CH_2-3), 1.63 (s, 3H, CH_3-4′), 1.61–1.53 (m, 2H, CH_2-1′), 1.26 (s, 3H, CH_3-2); ^{13}C NMR (75 MHz, $CDCl_3$) δ 168.5 (C-1‴), 162.4 (d, J_{CF} = 244 Hz, C-4″), 151.9 (C-6), 150.3 (C-2a‴), 148.2 (CH-7′), 147.6 (C-8a), 133.6 (C-4′), 133.2 (d, J_{CF} = 3 Hz, C-1″), 130.1 (C-6a‴), 129.3 (d, J_{CF} = 8 Hz, CH-2″, CH-6″), 125.9 (CH-4‴), 125.4 (CH-3′), 121.8 (CH-5‴), 121.7 (C-4a), 121.3 (CH-3‴), 119.0 (CH-6‴), 117.7 (CH-5), 115.3 (d, J_{CF} = 21 Hz, CH-5″, CH-3″), 115.2 (CH-7), 114.3 (CH-8), 75.6 (C-2), 70.0 (OCH_2Ph-*p*-F), 39.2 (CH_2-1′), 36.3 (CH_2-6′), 31.0 (CH_2-3), 30.7 (CH_2-5′), 24.1 (CH_3-2), 22.4 (CH_2-2′), 22.1 (CH_2-4), 15.9 (CH_3-4′); HRMS (ESI) *m/z* calcd for $C_{32}H_{35}FN_3O_2S$ [M+H] + 544.2429, found: 544.2409.

4.7.4. 5-Chloro-2-(2-7-(6-((p-fluorobenzyl)oxy)-2-methylbenzodihydropyran-2-yl)-4-methylhept -4-en-1-ylidene) hydrazineyl)-3-(trifluoromethyl)pyridine (14)

The title compound was prepared from aldehyde **12** (26.50 mg, 0.07 mmol) and 1-[5-chloro-3-(trifluoromethyl)-2-pyridyl]hydrazine (23.6 mg, 0.114 mmol) following the general procedure for the synthesis of compound **5**. The residue obtained was purified by silica gel column chromatography (CH_2Cl_2/MeOH, 98:2) to afford compound **14** (24.5 mg, 0.04 mmol, 59.5%) as a yellowish oil. ^{1}H NMR (300 MHz, $CDCl_3$) δ 8.42–8.40 (m, 1H, CH-6‴), 7.96 (brs, 1H, NH), 7.74–7.72 (m, 1H, CH-4‴), 7.40–7.36 (m, 2H, CH-2″, CH-6″), 7.28–7.26 (m, 1H, CH-7′), 7.08–7.02 (m, 2H, CH-3″, CH-5″), 6.72–6.65 (m, 3H, CH-5, CH-7, CH-8), 5.21–5.16 (m, 1H, CH-3′), 4.93 (s, 2H, OCH_2Ph-*p*-F), 2.74–2.70 (m, 2H, CH_2-4), 2.57–2.40 (m, 2H, CH_2-5′), 2.33–2.09 (m, 4H, CH_2-6′, CH_2-2′), 1.84–1.76 (m, 2H, CH_2-3), 1.74 (s, 3H, CH_3-4′), 1.73–1.56 (m, 2H, CH_2-1′), 1.27 (s, 3H, CH_3-2); ^{13}C NMR (75 MHz, $CDCl_3$) δ 162.4 (d, J_{CF} = 244 Hz, C-4″), 151.9 (C-6), 150.9 (q, J_{CF} = 4 Hz, CH-2‴), 148.4 (CH-7′), 148.2 (C-8a), 146.9 (CH-6‴), 135.2 (q, *J* = 4 Hz, CH-4‴), 135.5 (C-4′), 133.2 (d, J_{CF} = 3 Hz, C-1″), 129.2 (d, J_{CF} = 8 Hz, CH-2″, CH-6″), 125.4 (CH-3′), 123.4 (q, J_{CF}= 270 Hz, CF_3), 121.6 (C-4a), 121.2 (C-5‴), 117.7 (CH-5), 115.3 (d, J_{CF} = 21 Hz, CH-3″, CH-5″), 115.2 (CH-7), 114.3 (CH-8), 108.5 (q, J_{CF} = 33 Hz, C-3‴), 75.5 (C-2), 70.0 (OCH_2Ph-*p*-F), 39.1 (CH_2-1′), 36.7 (CH_2-6′), 31.0 (CH_2-3), 30.6 (CH_2-5′), 24.0 (CH_3-2), 22.4 (CH_2-2′), 22.1 (CH_2-4), 15.8 (CH_3-4′); HRMS (ESI) *m/z* calcd for $C_{31}H_{31}ClF_4N_3O_2$ [M − H] + 588.2040, found: 588.2017.

4.8. Evaluation of PPAR activity by transactivation assays

PPAR transcriptional activity of synthesized compounds was performed using a human chimera PPAR/Gal4 gene reporter luciferase system for each compound and compared with WY-14,643 (pirinixic acid, Sigma-Aldrich, St. Louis, MO) at 10 μM for PPARα, rosiglitazone (Sigma-Aldrich) at 1 μM for PPARγ and GW501516 (Sigma-Aldrich) at 1 μM for PPARβ/*δ*. Cos-7 cells (CRL-1651, ATCC, Manassas, VA) were maintained under standard culture conditions (Dulbecco's modified Eagle's minimal essential medium: DMEM supplemented with 10% fetal calf serum [FCS], Thermo Fisher Scientific, Waltham, MA) at 37 °C in a humidified atmosphere of 5% CO_2. The medium was changed every 2 days. Cells (5.5 Å∼ 105 cells/mL) were seeded in 60-mm dishes in DMEM supplemented with 10% FCS and incubated at 37 °C for 16 h prior to transfection. Cells were transfected in DMEM with the jetPEI transfection reagent (Polyplus-Transfection S.A., Strasbourg, France) using the reporter plasmid pG5-TK-pGL3 in combination with one of the expression plasmids, pGal4hPPARα, pGal4hPPARγ or pGal4hPPARβ/*δ*. The pCMV-β-galactosidase expression plasmid was included as a control of transfection efficiency. The transfection was stopped after 16 h by the addition of DMEM supplemented with 0.2% FCS, and cells were detached with trypsin and re-seeded in 96-well plates and incubated for 6 h in DMEM containing 0.2% FCS. Cells were then incubated for 24 h in DMEM containing 0.2% FCS and increasing concentrations of the compound tested or vehicle (DMSO, 0.1% final concentration). At the end of the experiment, cells were washed once with ice-cold phosphate buffered saline (PBS) and lysed, and luciferase and β-galactosidase activity were measured. Each experiment was achieved in triplicate, and mean ± standard error (SEM) values were calculated using GraphPad Prism 5 Software.

4.9. Molecular modelling

In molecular simulations for PPARα PPARγ and PPARδ receptors, we have used the same methodology as previously reported [20,24]. Docking calculations were carried out by using the Autodock 4.2 program [50] to localize the different ligands in the binding pocket; such complexes were used as starting structures for MD simulations. We used a molecular mechanics generalized born surface area (MM-GBSA) free energy decomposition analysis to determine the molecular interactions between the different ligands with PPARα PPAR-γ and PPARδ receptors. The 3D crystal structure of PPARγ in complex with rosiglitazone (PDB code: 4eMA) of PPARα in complex with WY-14643 (PDB code: 4BcR), and of PPARδ in complex with GW501516 (PDB code: 5U46) were used for MD simulations. The missing loop (261−275) in the PPARγ was modeled based on the 3D structure (PPARγ1PRG model) [51] using the Swiss-Model server [52]. Geometries of the complexes obtained from docking were soaked in boxes of explicit water using the TIP3P model and subjected to MD simulation. MD simulations were performed with the Amber 22 software package [52]. The geometry of the system went through a two-step energy minimization process: in the first step, the backbone atoms of the complex were constrained with 10.0 kcal/(mol Å2) force constants; in the second step, all solute and solvent atoms were allowed to move with no constraint to obtain the final relaxed geometry. The nonbonded interaction cutoff was kept at its default value, and the particle mesh Ewald method was also used. Simulations were performed with a total of 90 ns for each complex (three runs of 30 ns). The cluster process was carried out in the following manner: using the 90 ns obtained from three runs, 15 ns were discarded (the first 5 ns of each individual run). The remaining 75 ns were submitted to the cluster process, from which 10 different families of complexes were obtained. The free energy decomposition by residue was calculated using de *mm_pbsa* program in Amber22 [52]. Each ligand−residue pair includes four energy terms: van der Waals contribution (ΔEvdw), electrostatic contribution (ΔEele), polar desolvation term (ΔGGB), and nonpolar desolvation term (ΔGSA), which are summarized in the following equation: ΔGligand-residue = ΔEvdW + ΔEele + ΔGGB + ΔGSA.MD trajectories and the explicit water molecules were removed from the snapshots.

4.10. Study of anti-inflammatory activity

THP-1 human monocytes (ATCC, TIB-202™, Manassas, VA) were cultured in RPMI-1640 medium containing gentamycin (40 mg/mL), 1% (v/v) glutamine and 10% (v/v) fetal calf serum and maintained in a 37 °C, 5% CO_2 incubator. Cells (2×10^6 cells/mL) were seeded in 6-well

plates and were differentiated into macrophages by the addition of phorbol-12-myristate-13-acetate at 5 ng/mL (PMA, Promega). After 48 h, the cells were washed with PBS and replaced with 0% SVF medium for 1 h. After 1 h the depravation medium was replaced with stimulation medium containing hydrazones (**4**, **5** and **14** at 10 μM) or vehicle (<0.02% DMSO). The following hour, THP-1 macrophages were stimulated with LPS (100 ng/mL) in presence or not of PPAR activators hydrazones **4**, **5** and **14** at 10 μM, and secreted cytokine levels were measured 24 h later with ELISA kits according to the manufacturer's instructions (R&D System, Minneapolis, MN, USA). Cytokine mRNA levels were determined by quantitative PCR analysis.

4.11. Flow cytometry analysis of activated NF-κB

The effect of hydrazones **4** and **5** on LPS-induced NF-κB activation was determined in THP-1 cells by flow cytometry. THP-1 cells were incubated for 24 h with compounds (10 μM) or vehicle (0.02% DMSO) and then stimulated for 1 h with LPS 100 ng/mL.

Cells were then fixed and permeabilized using a commercial kit (Transcription Factor Phospho Buffer Set, 563239, BD Biosciences). Cells were then incubated with saturated amounts of a PE-conjugated monoclonal antibody against human NF-κB p65 (clone K10–895.12.50, IgG2B, BD Biosciences), for 45 min at 4 °C in the dark. Samples were run in a flow cytometer (BD LSRFortessa™ X-20, BD Biosciences). Results are presented as the mean fluorescence intensity of p65-NF-κB-expressing (PE fluorescence) THP-1.

4.12. Study of cytotoxic activity

THP-1 human monocytes (ATCC, TIB-202™, Manassas, VA) were cultured in RPMI-1640 medium containing gentamycin (40 mg/mL), 1% (v/v) glutamine and 10% (v/v) fetal calf serum and maintained in a 37 °C, 5% CO_2 incubator. Cells (1×10^5 cells/mL) were seeded in 24-well plates and were differentiated into macrophages by the addition of phorbol-12-myristate-13-acetate at 5 ng/mL (PMA, Promega). After 48 h, the cells were washed with PBS and replaced with the different compounds at 10 μM, 30 μM and 100 μM in complete medium or vehicle (<0.2% DMSO). Then, all cells were processes with Annexin V-assay kit (ANXCKF7, Inmunoestep, Salamanca, Spain) according to the manufacturer's instructions. BD LSR Fortessa cytometer (BD Biosciences, New Jersey, USA) was used for samples and cell analyses were performed by using BD FACSDiva X20 Software).

4.13. Statistical analysis

Data are presented as mean ± SEM. Statistical analyses were carried out by one-way or two-way ANOVA, followed by Tukey's or Dunnett's multiple comparisons test (GraphPad Prism 9). Paired analysis was performed by Wilcoxon matched-pairs signed rank test (GraphPad Prism 9). Differences with a p-value<0.05 were considered statistically different.

CRediT authorship contribution statement

Ainhoa García: Writing – original draft, Investigation, Formal analysis. **Laura Vila:** Methodology, Investigation, Formal analysis. **Isabelle Duplan:** Software, Methodology, Investigation, Formal analysis. **María Ayelén Schiel:** Software, Methodology, Investigation, Formal analysis. **Ricardo D. Enriz:** Validation, Supervision. **Nathalie Hennuyer:** Visualization, Validation, Supervision, Investigation. **Bart Staels:** Visualization, Supervision. **Nuria Cabedo:** Writing – review & editing, Writing – original draft, Supervision, Project administration, Funding acquisition, Data curation, Conceptualization. **Diego Cortes:** Validation, Supervision, Conceptualization.

Declaration of competing interest

The authors declare that they have no known competing financial interests or personal relationships that could have appeared to influence the work reported in this paper.

Data availability

No data was used for the research described in the article.

Acknowledgment

We are grateful for the financial support from Carlos III Health Institute (ISCIII) and the European Regional Development Fund (FEDER) (grants: PI18/01450 and PI21/0245), as well as Generalitat Valencia (APOTIP/2020/011 and AICO/2021/081). N.C. is an investigator in the 'Miguel Servet' programme (CPII20/00010) funded by the ISCIII and the European Social Fund. C.V. was funded by pre-doctoral PFIS grant from the ISCIII (FI19/00153).

Appendix A. Supplementary data

Supplementary data to this article can be found online at https://doi.org/10.1016/j.ejmech.2024.116125.

References

[1] B. Gross, M. Pawlak, P. Lefebvre, B. Staels, PPARs in obesity-induced T2DM, dyslipidaemia and NAFLD, Nat. Rev. Endocrinol. 13 (1) (2017) 36–49, https://doi.org/10.1038/nrendo.2016.135.
[2] C. Villarroel-Vicente, S. Gutiérrez-Palomo, J. Ferri, D. Cortes, N. Cabedo, Natural products and analogs as preventive agents for metabolic syndrome via peroxisome proliferator-activated receptors: an overview, Eur. J. Med. Chem. 221 (2021) 113535, https://doi.org/10.1016/j.ejmech.2021.113535.
[3] M. Dominguez, S. Alvarez, A.R. de Lera, Natural and structure-based RXR Ligand scaffolds and their functions, Curr. Top. Med. Chem. 17 (6) (2017) 631–662, https://doi.org/10.2174/1568026616666160617072521.
[4] T.M. Willson, P.J. Brown, D.D. Sternbach, B.R. Henke, The PPARs: from orphan receptors to drug discovery, J. Med. Chem. 43 (4) (2000) 527–550, https://doi.org/10.1021/jm990554g.
[5] O. Ziouzenkova, J. Plutzky, Retinoid metabolism and nuclear receptor responses: new insights into coordinated regulation of the PPAR-RXR complex, FEBS Lett. 582 (1) (2008) 32–38, https://doi.org/10.1016/j.febslet.2007.11.081.
[6] M. Pawlak, P. Lefebvre, B. Staels, Molecular mechanism of PPARα action and its impact on lipid metabolism, inflammation and fibrosis in non-alcoholic fatty liver disease, J. Hepatol. 62 (3) (2015) 720–733, https://doi.org/10.1016/j.jhep.2014.10.039.
[7] S.K. Ramakrishnan, L. Russo, S.S. Ghanem, P.R. Patel, A.M. Oyarce, G. Heinrich, S. M. Najjar, Fenofibrate decreases insulin clearance and insulin secretion to maintain insulin sensitivity, J. Biol. Chem. 291 (46) (2016) 23915–23924, https://doi.org/10.1074/jbc.M116.745778.
[8] F. Lalloyer, B. Vandewalle, F. Percevault, G. Torpier, J. Kerr-Conte, M. Oosterveer, R. Paumelle, J.C. Fruchart, F. Kuipers, F. Pattou, C. Fiévet, B. Staels, B, Peroxisome proliferator-activated receptor alpha improves pancreatic adaptation to insulin resistance in obese mice and reduces lipotoxicity in human islets, Diabetes 55 (6) (2006) 1605–1613, https://doi.org/10.2337/db06-0016.
[9] X. Palomer, E. Barroso, J. Pizarro-Delgado, L. Peña, G. Botteri, M. Zarei, D. Aguilar, M. Montori-Grau, M. Vázquez-Carrera, Pparβ/δ: a key therapeutic target in metabolic disorders, Int. J. Mol. Sci. 19 (3) (2018) 913, https://doi.org/10.3390/ijms19030913.
[10] L. Wang, B. Waltenberger, E.M. Pferschy-Wenzig, M. Blunder, X. Liu, C. Malainer, T. Blazevic, S. Schwaiger, J.M. Rollinger, E.H. Heiss, D. Schuster, B. Kopp, R. Bauer, H. Stuppner, V.M. Dirsch, A.G. Atanasov, Natural product agonists of peroxisome proliferator-activated receptor gamma (PPARγ): a review, Biochem. Pharmacol. 92 (1) (2014) 73–89, https://doi.org/10.1016/j.bcp.2014.07.018.
[11] S. Russo, M. Kwiatkowski, N. Govorukhina, R. Bischoff, B.N. Melgert, Meta-inflammation and metabolic reprogramming of macrophages in diabetes and obesity: the importance of metabolites, Front. Immunol. 12 (2021) 746151, https://doi.org/10.3389/fimmu.2021.746151.
[12] A.E. Boniakowski, A.S. Kimball, B.N. Jacobs, S.L. Kunkel, K.A. Gallagher, Macrophage-mediated inflammation in normal and diabetic wound healing, J. Immunol. 199 (1) (2017) 17–24, https://doi.org/10.4049/jimmunol.1700223.
[13] A. Chawla, Control of macrophage activation and function by PPARs, Circ. Res. 106 (10) (2010) 1559–1569, https://doi.org/10.1161/CIRCRESAHA.110.216523.
[14] T.L. Cranford, R.T. Enos, K.T. Velázquez, J.L. McClellan, J.M. Davis, U.P. Singh, M. Nagarkatti, P.S. Nagarkatti, C.M. Robinson, E.A. Murphy, Role of MCP-1 on inflammatory processes and metabolic dysfunction following high-fat feedings in

the FVB/N strain, Int. J. Obes. 40 (5) (2016) 844–851, https://doi.org/10.1038/ijo.2015.244.
[15] J. Panee, Monocyte chemoattractant protein 1 (MCP-1) in obesity and diabetes, Cytokine 60 (1) (2012) 1–12, https://doi.org/10.1016/j.cyto.2012.06.018.
[16] H. Kanda, S. Tateya, Y. Tamori, K. Kotani, K. Hiasa, R. Kitazawa, S. Kitazawa, H. Miyachi, S. Maeda, K. Egashira, M. Kasuga, MCP-1 contributes to macrophage infiltration into adipose tissue, insulin resistance, and hepatic steatosis in obesity, J. Clin. Invest. 116 (6) (2016) 1494–1505, https://doi.org/10.1172/JCI26498.
[17] D. Qu, J. Liu, C.W. Lau, Y. Huang, IL-6 in diabetes and cardiovascular complications, Br. J. Pharmacol. 171 (15) (2014) 3595–3603, https://doi.org/10.1111/bph.12713.
[18] D. Toobian, P. Ghosh, G.D. Katkar, Parsing the role of PPARs in macrophage processes, Front. Immunol. 12 (2021) 783780, https://doi.org/10.3389/fimmu.2021.783780.
[19] M.C. Gonzalez, A. Serrano, M.C. Zafra-Polo, D. Cortes, K.S. Rao, Polycerasoidin and polycerasoidol, two new prenylated benzopyran derivates from Polyalthia cerasoides, J. Nat. Prod. 58 (8) (1995) 1278–1284, https://doi.org/10.1021/np50122a022.
[20] A. Bermejo, A. Collado, I. Barrachina, P. Marqués, N. El Aouad, X. Franck, F. Garibotto, C. Dacquet, D.H. Caignard, F.D. Suvire, R.D. Enriz, L. Piqueras, B. Figadère, M.J. Sanz, N. Cabedo, D. Cortes, Polycerasoidol, a natural prenylated benzopyran with a dual PPARα/PPARγ agonist activity and anti-inflammatory effect, J. Nat. Prod. 82 (7) (2019) 1802–1812, https://doi.org/10.1021/acs.jnatprod.9b00003.
[21] A. García, L. Vila, P. Marín, Á. Bernabeu, C. Villarroel-Vicente, N. Hennuyer, B. Staels, X. Franck, B. Figadère, N. Cabedo, D. Cortes, Synthesis of 2-prenylated alkoxylated benzopyrans by horner-wadsworth-emmons olefination with PPARα/γ agonist activity, ACS Med. Chem. Lett. 12 (11) (2021) 1783–1786, https://doi.org/10.1021/acsmedchemlett.1c00400.
[22] L. Vila, N. Cabedo, C. Villarroel-Vicente, A. García, Á. Bernabeu, N. Hennuyer, B. Staels, X. Franck, B. Figadère, M.J. Sanz, D. Cortes, Synthesis and biological studies of "Polycerasoidol" and "trans-δ-Tocotrienolic acid" derivatives as PPARα and/or PPARγ agonists, Bioorg. Med. Chem. 53 (2022) 116532, https://doi.org/10.1016/j.bmc.2021.116532.
[23] A. Bermejo, I. Barrachina, N. El Aouad, X. Franck, N. Chahboune, I. Andreu, B. Figadère, L. Vila, N. Hennuyer, B. Staels, C. Dacquet, D.H. Caignard, M.J. Sanz, D. Cortes, N. Cabedo, Synthesis of benzopyran derivatives as PPARα and/or PPARγ activators, Bioorg. Med. Chem. 27 (24) (2019) 115162, https://doi.org/10.1016/j.bmc.2019.115162.
[24] P. Marques, C. Villarroel-Vicente, A. Collado, A. García, L. Vila, I. Duplan, N. Hennuyer, F. Garibotto, R.D. Enriz, C. Dacquet, B. Staels, L. Piqueras, D. Cortes, M.J. Sanz, N. Cabedo, Anti-inflammatory effects and improved metabolic derangements in ob/ob mice by a newly synthesized prenylated benzopyran with pan-PPAR activity, Pharmacol. Res. 187 (2023) 106638, https://doi.org/10.1016/j.phrs.2022.106638.
[25] L.M. Blair, J. Sperry, Natural products containing a nitrogen-nitrogen bond, J. Nat. Prod. 76 (4) (2013) 794–812, https://doi.org/10.1021/np400124n.
[26] M.A. El-Sayed, N.I. Abdel-Aziz, A.A. Abdel-Aziz, A.S. El-Azab, Y.A. Asiri, K. E. Eltahir, Design, synthesis, and biological evaluation of substituted hydrazone and pyrazole derivatives as selective COX-2 inhibitors: molecular docking study, Bioorg. Med. Chem. 19 (11) (2011) 3416–3424, https://doi.org/10.1016/j.bmc.2011.04.027.
[27] K. Pyta, A. Janas, M. Szukowska, P. Pecyna, M. Jaworska, M. Gajecka, F. Bartl, P. Przybylski, Synthesis, docking and antibacterial studies of more potent amine and hydrazone rifamycin congeners than rifampicin, Eur. J. Med. Chem. 167 (2019) 96–104, https://doi.org/10.1016/j.ejmech.2019.02.009.
[28] E.S. Coimbra, M.V. Nora de Souza, M.S. Terror, A.C. Pinheiro, J. da Trindade Granato, Synthesis, Biological activity, and mechanism of action of new 2-pyrimidinyl hydrazone and N-acylhydrazone derivatives, a potent and new classes of antileishmanial agents, Eur. J. Med. Chem. 184 (2019) 111742, https://doi.org/10.1016/j.ejmech.2019.111742.
[29] H. Lei, C. Li, Y. Yang, F. Jia, M. Guo, M. Zhu, N. Jiang, X. Zhai, Structure guided design of potent indole-based ATX inhibitors bearing hydrazone moiety with tumor suppression effects, Eur. J. Med. Chem. 201 (2020) 112456, https://doi.org/10.1016/j.ejmech.2020.112456.
[30] G. Pooja, S.R. Ravindra, B. Harshil, K. Sanjit, R.R. Sabbasani, Recent developments in the synthesis of N-heterocyclic compounds as α-amylase inhibitors via in-vitro and in-silico analysis: future drugs for treating diabetes, ChemistrySelect 7 (28) (2022), https://doi.org/10.1002/slct.202201706.
[31] J. Dowarah, V.P. Singh, Anti-diabetic drugs recent approaches and advancements, Bioorg. Med. Chem. 28 (5) (2020) 115263, https://doi.org/10.1016/j.bmc.2019.115263.
[32] D. Montaigne, L. Butruille, B. Staels, PPAR control of metabolism and cardiovascular functions, Nat. Rev. Cardiol. 18 (12) (2021) 809–823, https://doi.org/10.1038/s41569-021-00569-6.
[33] E.B. Lindgren, M.A. de Brito, T.R. Vasconcelos, M.O. de Moraes, R.C. Montenegro, J.D. Yoneda, K.Z, Synthesis and anticancer activity of (E)-2-benzothiazole hydrazones, Eur. J. Med. Chem. 86 (2014) 12–16, https://doi.org/10.1016/j.ejmech.2014.08.039.
[34] J. Párraga, L. Moreno, A. Diaz, N. El Aouad, A. Galán, M.J. Sanz, D.H. Caignard, B. Figadère, N. Cabedo, D. Cortes, Efficient synthesis of hexahydroindenopyridines and their potential as melatoninergic ligands, Eur. J. Med. Chem. 86 (2014) 700–709, https://doi.org/10.1016/j.ejmech.2014.09.038.
[35] Q.P. Peterson, D.C. Hsu, D.R. Goode, C.J. Novotny, R.K. Totten, P.J. Hergenrother, Procaspase-3 activation as an anti-cancer strategy: structure-activity relationship of procaspase-activating compound 1 (PAC-1) and its cellular co-localization with caspase-3, J. Med. Chem. 52 (18) (2009) 5721–5731, https://doi.org/10.1021/jm900722z.
[36] Y. Yang, L. Shouxin, L. Junzhang, T. Xia, Z. Xiaoli, H. Jianrong, Convenient method for reduction of C-N double bonds in oximes, imines, and hydrazones using sodium borohydride–raney Ni system, Synth. Commun. 42 (17) (2012) 2540–2554, https://doi.org/10.1080/00397911.2011.562063.
[37] M. Krátký, Š. Štěpánková, K. Konečná, K. Svrčková, J. Maixnerová, M. Švarcová, O. Janďourek, F. Trejtnar, J. Vinšová, Novel aminoguanidine hydrazone analogues: from potential antimicrobial agents to potent cholinesterase inhibitors, Pharmaceuticals 14 (12) (2021) 1229, https://doi.org/10.3390/ph14121229.
[38] D. Perdicchia, L. Emanuela, M. Estefano, B. Clara, G. Clelia, A new 'one-pot' synthesis of hydrazides by reduction of hydrazones, Tetrahedron 59 (39) (2003) 7733–7742, https://doi.org/10.1016/S0040-4020(03)01208-0.
[39] J.M. Khurana, B.M. Kandpal, P. Sharma, M. Gupta, A novel method of reduction of C=N-group in hydrazones, phenylhydrazones, azines, and tosylhydrazones by Mg–methanol, Monatshefte für Chemie - Chemical Monthly 146 (1) (2015) 187–190, https://doi.org/10.1007/s00706-014-1306-6.
[40] A. Srikrishna, T.J. Reddy, R. Viswajanani, Reduction of quinolines to 1,2,3,4-tetrahydro derivatives employing a combination of $NaCNBH_3$ and BF_3, OEt_2. Tetrahedron 52 (5) (1996) 1631–1636, https://doi.org/10.1016/0040-4020(95)00991-4.
[41] J. Kalia, R.T. Raines, Hydrolytic stability of hydrazones and oximes, Angew. Chem. Int. Ed. Engl. 47 (39) (2008) 7523–7526, https://doi.org/10.1002/anie.200802651.
[42] R R Kshirsagar, P.K. Gadekar, V.M. Khedkar, V. Vijayakumar, Design, synthesis, and the Effects of (*E*)-9-oxooctadec-10-en-12-ynoic acid analogues to promote glucose uptake, ACS Omega 6 (37) (2021) 24118–24127, https://doi.org/10.1021/acsomega.1c03600.
[43] T. Kato, K. Fukao, T. Ohara, N. Naya, R. Tokuyama, S. Muto, H. Fukasawa, A. Itai, K.I. Matsumura, Design, synthesis, and anti-inflammatory evaluation of a novel PPARδ agonist with a 4-(1-pyrrolidinyl)piperidine Structure, J. Med. Chem. 66 (16) (2023) 11428–11446, https://doi.org/10.1021/acs.jmedchem.3c00932.
[44] M. Di Stefano, S. Masoni, G. Bononi, G. Poli, S. Galati, F. Gado, S. Manzi, C. Vagaggini, A. Brai, I. Caligiuri, K. Asif, F. Rizzolio, M. Macchia, A. Chicca, A. Sodi, V. Di Bussolo, F. Minutolo, P. Meier, J. Gertsch, C. Granchi, E. Dreassi, T. Tuccinardi, Design, synthesis, ADME and biological evaluation of benzylpiperidine and benzylpiperazine derivatives as novel reversible monoacylglycerol lipase (MAGL) inhibitors, Eur. J. Med. Chem. 263 (2023) 115916, https://doi.org/10.1016/j.ejmech.2023.115916. Advance online publication.
[45] A. Bernardes, P.C. Souza, J.R. Muniz, C.G. Ricci, S.D. Ayers, N.M. Parekh, A. S. Godoy, D.B. Trivella, P. Reinach, P. Webb, M.S. Skaf, I. Polikarpov, Molecular mechanism of peroxisome proliferator-activated receptor α activation by WY14643: a new mode of ligand recognition and receptor stabilization, J. Mol. Biol. 425 (16) (2013) 2878–2893, https://doi.org/10.1016/j.jmb.2013.05.010.
[46] H.E. Xu, T.B. Stanley, V.G. Montana, M.H. Lambert, B.G. Shearer, J.E. Cobb, D. D. McKee, C.M. Galardi, K.D. Plunket, R.T. Nolte, D.J. Parks, J.T. Moore, S. A. Kliewer, T.M. Willson, J.B. Stimmel, Structural basis for antagonist-mediated recruitment of nuclear co-repressors by PPARalpha, Nature 415 (6873) (2002) 813–817, https://doi.org/10.1038/415813a.
[47] I. Kouskoumvekaki, R.K. Petersen, F. Fratev, O. Taboureau, T.E. Nielsen, T. L. Oprea, S.B. Sonne, E.N. Flindt, S.Ó. Jónsdóttir, K. Kristiansen, Discovery of a novel selective PPARγ ligand with partial agonist binding properties by integrated in silico/in vitro work flow, J. Chem. Inf. Model. 53 (4) (2013) 923–937, https://doi.org/10.1021/ci3006148.
[48] M.V. Liberato, A.S. Nascimento, S.D. Ayers, J.Z. Lin, A. Cvoro, R.L. Silveira, L. Martínez, P.C. Souza, D. Saidemberg, T. Deng, A.A. Amato, M. Togashi, W. A. Hsueh, K. Phillips, M.S. Palma, F.A. Neves, M.S. Skaf, P. Webb, I. Polikarpov, Medium chain fatty acids are selective peroxisome proliferator activated receptor (PPAR) γ activators and pan-PPAR partial agonists, PLoS One 7 (5) (2012) e36297, https://doi.org/10.1371/journal.pone.0036297.
[49] C.C. Wu, T.J. Baiga, M. Downes, J.J. La Clair, A.R. Atkins, S.B. Richard, W. Fan, T. A. Stockley-Noel, M.E. Bowman, J.P. Noel, R.M. Evans, Structural basis for specific ligation of the peroxisome proliferator-activated receptor δ, Proc. Natl. Acad. Sci. U S A 114 (13) (2017) E2563–E2570, https://doi.org/10.1073/pnas.1621513114.
[50] G.M. Morris, R. Huey, W. Lindstrom, M.F. Sanner, R.K. Belew, D.S. Goodsell, A. J. Olson, AutoDock4 and AutoDockTools4: automated docking with selective receptor flexibility, J. Comput. Chem. 30 (16) (2009) 2785–2791, https://doi.org/10.1002/jcc.21256.
[51] R.T. Nolte, G.B. Wisely, S. Westin, J.E. Cobb, M.H. Lambert, R. Kurokawa, M. G. Rosenfeld, T.M. Willson, C.K. Glass, M.V. Milburn, Ligand binding and co-activator assembly of the peroxisome proliferator-activated receptor-gamma, Nature 395 (6698) (1998) 137–143, https://doi.org/10.1038/25931.
[52] D.A. Case, H.M. Aktulga, K. Belfon, I.Y. Ben-Shalom, J.T. Berryman, S.R. Brozell, D. S. Cerutti, T.E. Cheatham III, G.A. Cisneros, V.W.D. Cruzeiro, T.A. Darden, N. Forouzesh, G. Giambaşu, T. Giese, M.K. Gilson, H. Gohlke, A.W. Goetz, J. Harris, S. Izadi, S.A. Izmailov, K. Kasavajhala, M.C. Kaymak, E. King, A. Kovalenko, T. Kurtzman, T.S. Lee, P. Li, C. Lin, J. Liu, T. Luchko, R. Luo, M. Machado, V. Man, M. Manathunga, K.M. Merz, Y. Miao, O. Mikhailovskii, G. Monard, H. Nguyen, K. A. O'Hearn, A. Onufriev, F. Pan, S. Pantano, R. Qi, A. Rahnamoun, D.R. Roe, A. Roitberg, C. Sagui, S. Schott-Verdugo, A. Shajan, J. Shen, C.L. Simmerling, N. R. Skrynnikov, J. Smith, J. Swails, R.C. Walker, J. Wang, J. Wang, H. Wei, X. Wu, Y. Wu, Y. Xiong, Y. Xue, D.M. York, S. Zhao, Q. Zhu, P.A. Kollman, Amber, University of California, San Francisco, 2023.